

12

AD A112701

AFAPL-TR-78-81
Volume II

FOREIGN OBJECT IMPACT DESIGN CRITERIA

Albert F. Storace

General Electric Company
Aircraft Engine Group
Cincinnati, Ohio 45215



February 1982

Interim Report for Period 31 December 1977 - 31 December 1978

Approved for public release; distribution unlimited.

DTIC FILE COPY

AERO PROPULSION LABORATORY
AIR FORCE WRIGHT AERONAUTICAL LABORATORIES
AIR FORCE SYSTEMS COMMAND
WRIGHT-PATTERSON AIR FORCE BASE, OHIO 45433

DTIC
ELECTE
MAR 22 1982
B

82 03 22 001

NOTICE

When Government drawings, specifications, or other data are used for any purpose other than in connection with a definitely related Government procurement operation, the United States Government thereby incurs no responsibility nor any obligation whatsoever, and the fact that the Government may have formulated, furnished, or in any way supplied the said drawings, specifications, or other data, is not to be regarded by implication or otherwise as in any manner licensing the holder or any other person or corporation, or conveying any rights or permission to manufacture, use, or sell any patented invention that may in any way be related thereto.

This technical report has been reviewed and is approved for publication.

Sandra K. Drake
SANDRA DRAKE
Project Engineer

Isak Z. Gershon
ISAK Z. GERSHON
Technical Area Manager,
Propulsion Mechanical Design

FOR THE COMMANDER:

James Shipman
J. SHIPMAN, MAJ, USAF
Chief, Components Branch

If your address has changed, if you wish to be removed from our mailing list, or if the addressee is no longer employed by your organization, please notify AFWAL/POTC WPAFB, OH 45433 to help us maintain a current mailing list.

Copies of this report should not be returned unless return is required by security considerations, contractual obligations, or notice on a specific document.

UNCLASSIFIED

SECURITY CLASSIFICATION OF THIS PAGE (When Data Entered)

REPORT DOCUMENTATION PAGE		READ INSTRUCTIONS BEFORE COMPLETING FORM								
1. REPORT NUMBER AFAPL-TR-78-81, VOL II	2. GOVT ACCESSION NO. AD-A112701	3. RECIPIENT'S CATALOG NUMBER								
4. TITLE (and Subtitle) FOREIGN OBJECT IMPACT DESIGN CRITERIA		5. TYPE OF REPORT & PERIOD COVERED Interim Technical Report 31 Dec. 1977 - 31 Dec. 1978								
		6. PERFORMING ORG. REPORT NUMBER R78AEG180								
7. AUTHOR(s) Albert F. Storace		8. CONTRACT OR GRANT NUMBER(s) F33615-77-C-5221								
9. PERFORMING ORGANIZATION NAME AND ADDRESS General Electric Company Aircraft Engine Group Cincinnati, Ohio 45215		10. PROGRAM ELEMENT, PROJECT, TASK AREA & WORK UNIT NUMBERS 3066-12-33								
11. CONTROLLING OFFICE NAME AND ADDRESS Aero Propulsion Laboratory (AFWAL/POTC) Air Force Wright Aeronautical Laboratories Wright-Patterson Air Force Base, Ohio 45433		12. REPORT DATE February 1982								
14. MONITORING AGENCY NAME & ADDRESS (if different from Controlling Office)		13. NUMBER OF PAGES 72								
		15. SECURITY CLASS. (of this report) Unclassified								
		15a. DECLASSIFICATION/DOWNGRADING SCHEDULE								
16. DISTRIBUTION STATEMENT (of this Report) Approved for public release; distribution unlimited.										
17. DISTRIBUTION STATEMENT (of the abstract entered in Block 20, if different from Report)										
18. SUPPLEMENTARY NOTES The computer program contained in this technical report is theoretical and in no way reflects any Air Force owned software programs.										
19. KEY WORDS (Continue on reverse side if necessary and identify by block number) <table border="0"> <tr> <td>Transient Structural Response</td> <td>Fan/Compressor Blad^e</td> </tr> <tr> <td>Foreign Object Loading</td> <td>Material Transient</td> </tr> <tr> <td>FOD Design Criteria</td> <td>Structural Failure</td> </tr> <tr> <td>Damage-Tolerant Design</td> <td>Airfoil Structural Modeling</td> </tr> </table>			Transient Structural Response	Fan/Compressor Blad ^e	Foreign Object Loading	Material Transient	FOD Design Criteria	Structural Failure	Damage-Tolerant Design	Airfoil Structural Modeling
Transient Structural Response	Fan/Compressor Blad ^e									
Foreign Object Loading	Material Transient									
FOD Design Criteria	Structural Failure									
Damage-Tolerant Design	Airfoil Structural Modeling									
20. ABSTRACT (Continue on reverse side if necessary and identify by block number) <p>The program objective is to establish specific design criteria and provide the analytical design tools to assess and improve the foreign object damage tolerance of turbine engine fan and compressor blading.</p> <p>This program will aid in the design of more efficient damage-tolerant blading through the replacement of trial and error FOD test and evaluation practices with systematic transient structural analysis methods, test procedures and design criteria.</p>										

DD FORM 1473
1 JAN 73

EDITION OF 1 NOV 65 IS OBSOLETE

UNCLASSIFIED

SECURITY CLASSIFICATION OF THIS PAGE (When Data Entered)

UNCLASSIFIED

SECURITY CLASSIFICATION OF THIS PAGE(When Data Entered)

A design system structure was completed and initial versions of the preliminary and final design transient structural response computer programs were developed. In addition, the interface between the bird loading model and the final design response model was completed. Three first stage blades were selected for modeling and testing. Tests and analyses to be used to generate local and gross structural damage design data are in progress and planning was completed for structural element impact tests. Composite and metallic specimens for local and gross damage testing were designed and most of these specimens have been fabricated. A parametric matrix to guide the analyses and validation testing was completed and FOD design criteria goals were formulated for consideration in the program.

UNCLASSIFIED

SECURITY CLASSIFICATION OF THIS PAGE(When Data Entered)

PREFACE

This report covers work performed by the Aircraft Engine Group at General Electric, Evendale, Ohio. This report covers work completed during the period 1 January 1978 through 31 December 1978. The contract, F33615-77-C-5221 was sponsored by the Aero Propulsion Laboratory, Air Force Systems Command, Wright-Patterson AFB, Ohio 45433, under Program Element 62203F, Project 3066, Task Area 12, Work Unit 33 and under the direction of Sandra K. Drake (AFWAL/POTC), Project Engineer. Albert F. Storace was technically responsible for the work and preparation of this report in fulfillment of the aforementioned contract.



Accession For	
NTIS GRA&I	<input checked="" type="checkbox"/>
DTIC TAB	<input type="checkbox"/>
Unannounced	<input type="checkbox"/>
Justification	
By _____	
Distribution/ _____	
Availability Codes	
Dist	Avail and/or Special
A	

TABLE OF CONTENTS

<u>Section</u>		<u>Page</u>
1.0	INTRODUCTION	1
2.0	SUMMARY	2
3.0	TASK I - DESIGN SYSTEM STRUCTURE	3
4.0	TASK II - TRANSIENT RESPONSE ANALYSIS MODELS	6
4.1	Introduction	6
4.2	First-Level Response Model (NOSAPM)	7
4.3	Second-Level Response Model (COMET-BLADE)	11
4.4	Interface With the Loading Model	11
5.0	TASK III - IMPACT LOADING MODEL	15
5.1	Introduction	15
5.2	Subtask A - Simulate Bird and Ice Impact Parameter	15
5.3	Subtask B - Loading Model Sensitivity Study	15
5.4	Subtask C - Formulation/Interfacing of Loading Models With Structural Models	17
5.4.1	Introduction	17
5.4.2	The Slicing Model	18
5.4.2.1	Slicing Model Development for Birds	18
5.4.2.2	Slice Geometry Parametric Study	22
5.4.3	Fluid Flow Model of Impact	22
5.4.3.1	Surface Singularity Method - Superposition of Onset Flow and Surface Source Distribution	23
5.4.3.2	The Body Surface Approximation	23
5.4.3.3	Solution Procedure	23
5.4.3.4	Onset Flow Modeling	24
5.4.4	Structure of the Loading Model and Interface With Response Models	24
5.4.5	Summary	26
5.5	Subtask D - Experimental Verification Loading Model	26
6.0	TASK IV - MATERIAL RESPONSE AND FAILURE CRITERIA	28
6.1	Subtask A - Gross Structural Damage Properties	28
6.1.1	Introduction	28
6.1.2	Real Blade Strain Rate	29
6.1.3	Material Property Data	31
6.2	Subtask B - Local Leading Edge Damage	41
6.2.1	Introduction	41
6.2.2	Overall Approach	43
6.2.3	Metal Specimen Tests	43

TABLE OF CONTENTS (Concluded)

<u>Section</u>	<u>Page</u>
6.2.4 Composite Specimen Tests	44
6.2.4.1 Laboratory Size Composite Specimen Tests	44
6.2.4.2 Full-Scale Composite Blade Tests	44
6.3 Subtask C - Material Screening Tests	44
6.3.1 Introduction	44
6.3.2 Materials to be Investigated	45
6.3.3 Screening Tests	45
6.3.3.1 Ballistic Limit Testing	45
6.3.3.2 Maximum Deformation Testing	46
6.3.3.3 Gross Structural Damage Testing	46
6.3.3.4 Fatigue Testing	46
7.0 TASK V - PARAMETRIC ANALYSIS	47
7.1 Introduction	47
7.2 Blades Selected for Analysis	47
7.3 Parametric Matrix	47
7.4 Modeling of the Structural Specimens	51
8.0 TASK VI - STRUCTURAL ELEMENT TESTS	56
8.1 Introduction	56
8.2 Composite Specimen Tests	56
8.2.1 Laboratory Size Composite Specimen Tests	56
8.2.2 Full-Scale Composite Blade Tests	58
8.3 Metal Specimen Tests	58
9.0 TASK VII - ERROR BAND ANALYSIS	61
9.1 Introduction	61
9.2 Properties Requiring an Error Band Estimation	61
10.0 TASK VIII - FOREIGN OBJECT IMPACT DESIGN CRITERIA	63
10.1 Introduction	63
10.2 Foreign Object Impact Design Criteria Goals	63
11.0 REFERENCES	64

LIST OF ILLUSTRATIONS

<u>Figure No.</u>		<u>Page</u>
1.	Program/Tasks Flow - Foreign Object Impact Design Data.	4
2.	Foreign Object Impact Design Criteria Program Functional Organization.	5
3(a).	Level 1 Response Model Formulated With 3-D Finite Elements.	8
3(b).	3-D Finite Element Used in NOSAPM.	9
4.	Plate Modeled From NOSAPM With 20-Noded Elements Rotating at 5000 RPM and Loaded With a Transient Load.	10
5.	Level 2 Transient Response Model Formulated From a System of Plate Elements.	12
6.	Link-up Between the Loading Model Subroutine and the Executive or Main Response Model Program.	14
7.	Loading Model Sensitivity Study 9-Element 20-Noded Brick Model of Cantilever Plate Using Symmetry.	16
8.	Bird-Blade/Interaction Geometry.	19
9.	Impact Test Setup for Real Blades.	30
10.	J79 Stage 1 Compressor Blade Strain Gage Locations for Maximum Strain Rate Determination.	31
11.	Strain and Strain Rate Time Histories for Gage No. 1 (at Root of Airfoil on Pressure Side).	32
12.	Strain and Strain Rate Time Histories for Gage No. 3.	33
13.	Strain in the Time and Frequency Domain Resulting from Hammer Blow for Gage No. 4 J79 Blade, Test Date 10/16/78.	34
14.	Tensile Specimen for Metals.	37
15.	Split Hopkinson Bar Specimen.	38
16.	Modified ITTRI Specimen.	39
17.	Modified 10° Off-Axis Shear Specimen.	40
18.	Through-the-Thickness Test Specimen.	42
19.	Comparison of 20-Noded Finite Element Solution With Beam Theory.	53
20.	Comparison of 16-Noded Finite Element Solution With 20-Noded Element Solution.	54
21.	Task VI B/A1 Composite Test Specimen Configurations.	57

LIST OF TABLES

<u>Table No.</u>		<u>Page</u>
1.	Blade Calculation Input Data Sheet for 3-Ounce Bird.	20
2.	Blade Calculation Input Data Sheet for 1.5-Pound Bird.	21
3.	Characterization of Metallic Materials.	36
4.	Characterization Tests for B/Al and Stainless Steel Wire Mesh.	41
5.	Parametric Matrix Defining Structural Elements and Impact Conditions to be Analyzed.	48
6.	Shape, Size and Configuration Details of Structural Elements.	52
7.	Task VI Fabricated Composite Specimen Test Conditions.	56
8.	Task VI - Real Composite Blade Test Conditions.	58
9.	Task VI - Fabricated Metal Specimen Test Conditions.	59
10.	Task VI - Real Metal Blade Test Conditions.	60
11.	Matrix of Error Band Properties and Associated Damage Modes.	62

1.0 INTRODUCTION

The objective of this program is to develop and validate structural design criteria that account for the transient overloads produced by bird and ice impacts on turbine engine first-stage fan/compressor blades. This program is part of a continuing effort of the Air Force to minimize ownership costs by placing added emphasis on the derivation of durable damage-tolerant advanced turbomachinery component designs.

Foreign object damage (FOD) in aircraft engines has been an increasing drain on defense economic resources. Present generation engine blading designs have substantial material toughness and cross section to meet the mechanical and aeromechanical requirements, but they were not specifically designed for damage tolerance. The prevailing design state-of-the-art concerning damage-tolerant blading is mostly empirical and based on experience from major incidents and associated ad hoc testing. The empirical approach to designing damage-tolerant blading requires considerable investment of resources and is sometimes incapable of providing directly predictable foreign object impact response of blading. This approach is not adequate for newer, more damage-prone blading designs incorporating lightweight materials, including advanced composites, and thinner cross sections to achieve improved performance.

To achieve more efficient damage-tolerant blading, comprehensive foreign object impact design criteria, based upon transient structural response tools, are needed. These tools will provide direct assessment of a blade's impact damage tolerance and identify areas for improvement. The purpose of this program is to provide the necessary computer tools and validation testing to establish reliable foreign object impact design criteria.

This program consists of 11 tasks which progressively develop the FOD design criteria from computer models, structural element and material property tests, and static and rotating single-blade tests to full- or partial-stage rotating tests. The 11 tasks are identified as follows:

- Task I - Design System Structure
- Task II - Transient Response Analysis Models
- Task III - Impact Loading Model
- Task IV - Material Response and Failure Criteria
- Task V - Parametric Analysis
- Task VI - Structural Element Tests
- Task VII - Error Band Analysis
- Task VIII - Foreign Object Impact Design Criteria
- Task IX - Single-Blade Impact Tests
- Task X - Full-Stage Response Prediction
- Task XI - Full-Scale Impact Tests

The design analysis methods and failure criteria derived in the course of this program will be applicable to both advanced composite materials and monolithic materials of construction for current and advanced fan/compressor blading.

2.0 SUMMARY

The program consists of 11 tasks to establish reliable foreign object impact design criteria. The emphasis will be on determining the effects of the ingestion of birds and ice during takeoff and landing, which present the greatest hazards to aircraft engines.

The 11 tasks progressively develop the FOD design criteria from transient structural response computer models, test specimens and single-blade tests to full- or partial-stage rotating rig tests. The transient response computer models will be based on existing mathematical approaches and on existing computing programs that will be adjusted as required for the specific application of this study.

Task I which develops a design structure for the purposes of providing a consistent framework in which to constitute the design criteria, guiding the overall technical effort and formulating a data foundation to define the problem environment has been completed.

Tasks II through VIII are currently underway and address to the development of the transient response and loading models, local and structural impact testing, material property determination, error band analysis and the formulation of design criteria.

Initial versions of the preliminary and final design transient structural response computer programs have been developed and checked out. In addition, the coding for interfacing the bird loading model developed by the University of Dayton Research Institute with the final design response model developed by General Electric has been completed and is in the final checkout stage.

Three first stage blades were selected for modeling and structural testing. Composite and metallic specimens for local impact and structural element bench impact and material property tests were designed and most of these specimens have been fabricated. Test plans defining the testing of these specimens and real blades have been completed and approved by the Air Force. Real blade impact testing to establish the maximum strain rates that are needed for the material property tests has been completed.

A parametric matrix to define the conditions and geometries that will be analyzed in Tasks V and X, and to provide guidance in the selection of the structural tests that will be conducted in Tasks VI and IX, has been formulated.

Work was started on the compilation of relevant blade and impactor properties for use in the error band analysis. FOD design criteria goals were established within the framework of the projected capabilities of the transient structural analysis computer tools being developed in Tasks II and III.

3.0 TASK I - DESIGN SYSTEM STRUCTURE

A design system structure was developed through the Task I effort to establish a consistent framework in which to constitute FOD design criteria and guide the overall technical effort. This design system structure defines the objective and interfaces of the various multidisciplined tasks that must be satisfied to achieve meaningful design criteria and includes a data foundation that describes the problem environment.

Figure 1 depicts the interrelations between the major distinct activities of quantification of experience, analytic development, bench tests, rotating rig tests, and the work flow of the program.

The results of the Task I effort were documented in a Research/Development Test Plan¹ that was approved by the Air Force.

To conduct the program described in Figure 1, a team of technical personnel has been gathered from several organizations to utilize their specific technical expertise and foreign object impact experience. These organizations are:

- General Electric Aircraft Engine Group (AEG)
- General Electric Corporate Research and Development Center (CR&DC)
- University of Dayton Research Institute (UDRI)

Figure 2 shows the functional responsibilities of the participants.

*Superscript numbers refer to references.

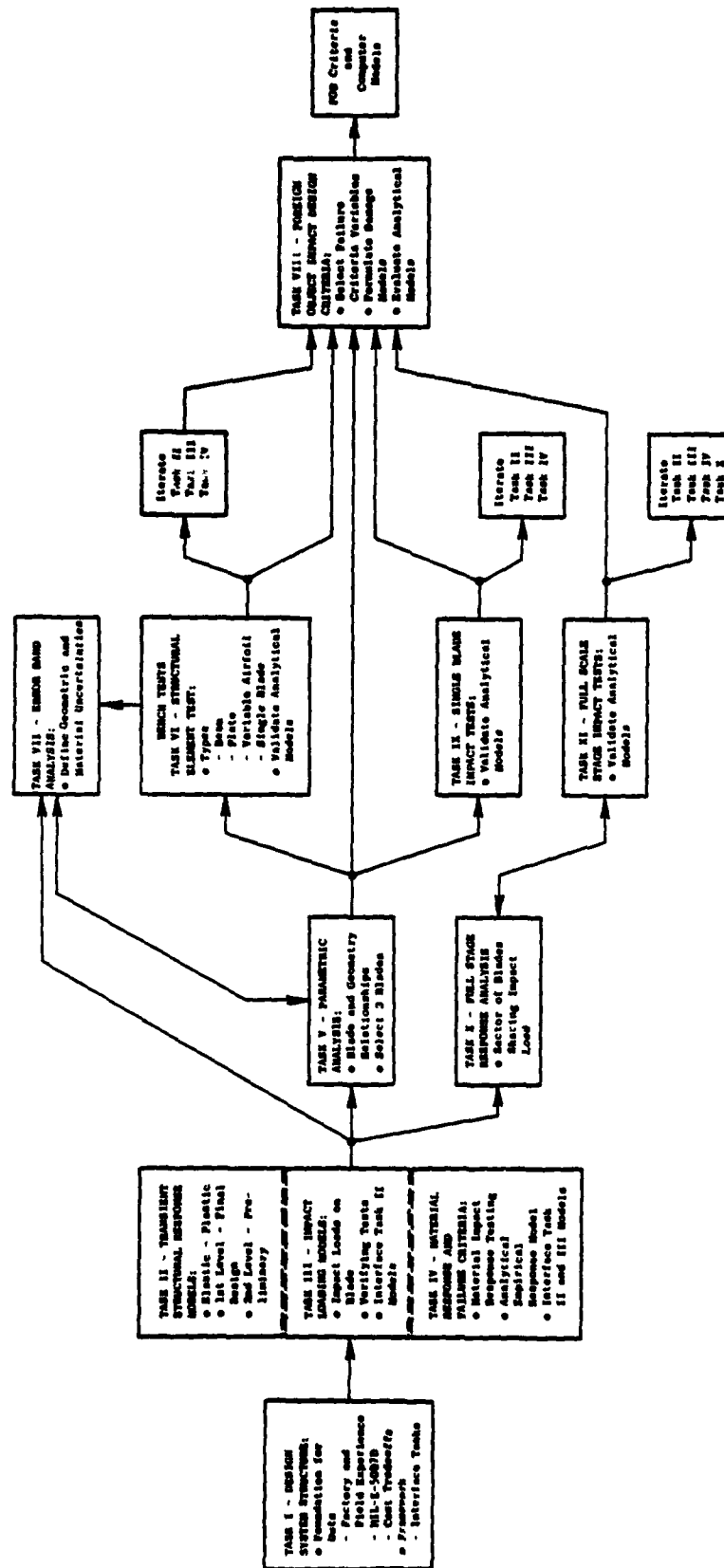


Figure 1. Program/Tasks Flow - Foreign Object Impact Design Criteria.

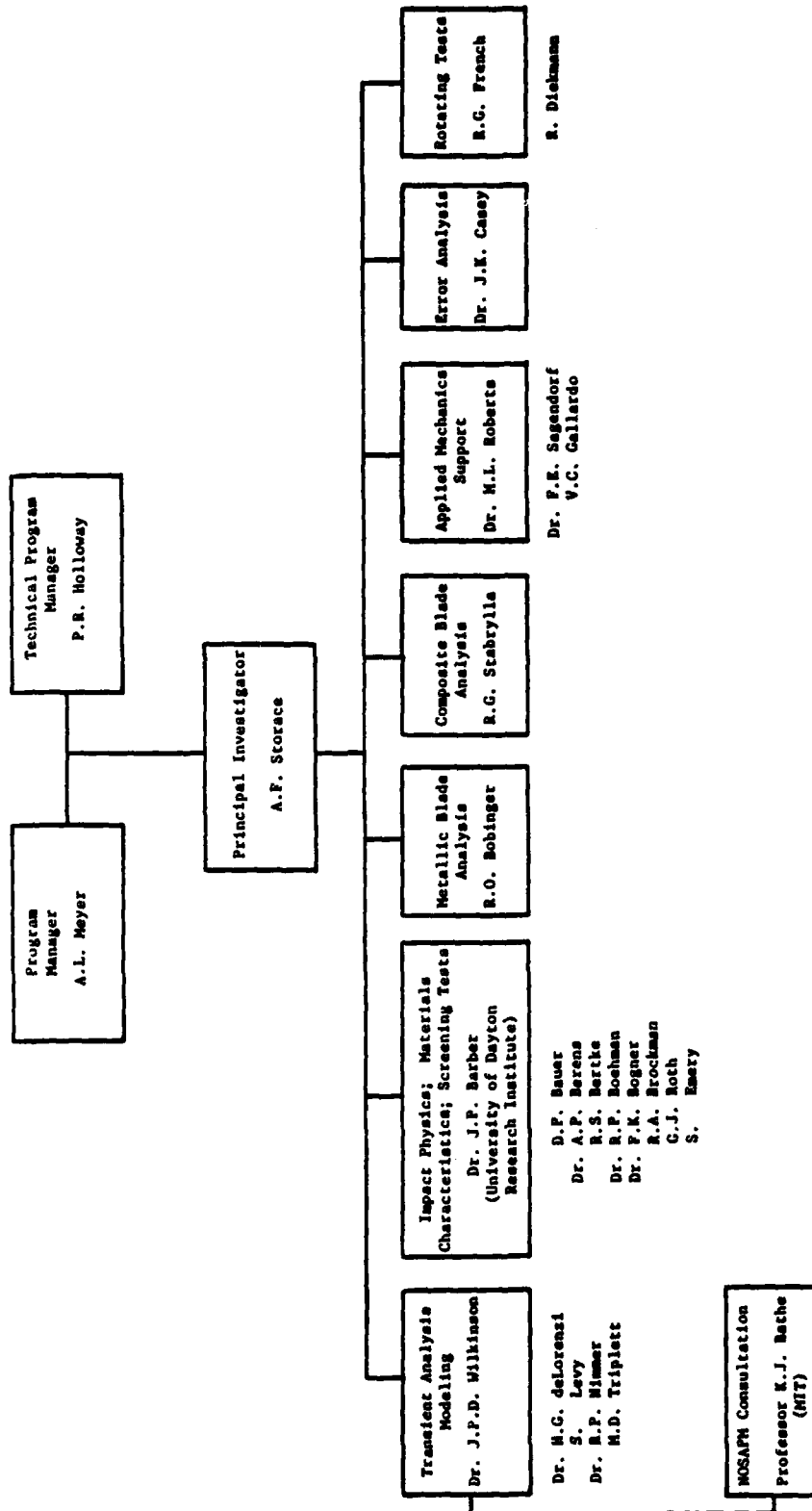


Figure 2. Foreign Object Impact Design Criteria Program Functional Organization.

4.0 TASK II - TRANSIENT RESPONSE ANALYSIS MODELS

The first- and second-level models² selected for use in the transient response analysis of first stage fan and compressor blades were approved by the Air Force.

4.1 INTRODUCTION

The transient response of first stage fan and compressor blades due to foreign object impact will be analyzed on two different levels during the course of this program. The rationale for this approach is based on the fact that each of the levels of analysis possess intrinsic advantages which make them very attractive for the study of different aspects of the FOD problem. The first level of analysis will be accomplished with a modified version of the finite element program NONSAP. This analysis will be capable of carrying out a very detailed analysis embracing local impact damage as well as gross structural damage. NONSAP is a very general and accurate package for non-linear, finite element analyses and contains 3-D elements which will be used herein. The modified version which will be used in this program will be called NOSAPM. This program has a library of three different time integration techniques (Wilson θ , Newmark, central difference) as well as two elasto-plastic hardening models (kinematic hardening and isotropic hardening). This versatility will prove useful in finding the most efficient strategy for solution of the dynamic problem. However, the detail and versatility of this NONSAP package is obtained at the expense of high computing costs which could prove to be a problem during parametric design studies. As a result, the second level analysis based on S. Levy's component element method of transient dynamics³ will be employed in these situations where cost becomes an important factor. The savings in the Component Element Method (COMET) are accomplished through the use of simplified element models and an explicit time integration technique which allows nonlinear structural dynamics problems to be solved without ever physically assembling stiffness matrices. This Level 2 analysis will be somewhat less detailed, but experience in other fields including pipe whip⁴, locomotive dynamics, and nuclear fuel rod vibration⁵ shows that the technique is as accurate as well as efficient tool. In addition to being of use in parametric studies, the lower cost of this level of analysis should prove to be an advantage in blade-interaction studies.

No dynamic crack growth analyses will be incorporated into the first and second level analyses. Stresses and strains will simply be calculated and then used to indicate damage based on the design criteria to be formed as part of Task VIII. Plastic curlback of blades will be considered. Graphical output of stresses and strains will be provided, and a method of implementing the results of the impact damage design criteria within the structural codes will be incorporated. Based on the transient response models of Task II and the damage criteria formulated in Task VIII, the final package would then indicate probable areas of failure as they are encountered in the analysis.

4.2 FIRST-LEVEL RESPONSE MODEL (NOSAPM)

As indicated above, the program NOSAPM contains a wide range of tools which will be necessary in modeling the FOD problem. Specifically, in this analysis, the 3-D isoparametric element will be used. This element can be used with a variable number of nodal points ranging from 8 to 21. It is anticipated that either 16 noded or 20 noded elements will be used to allow the blades to be modeled with one element through the thickness while still including the bending effects which will be most important in this problem. NOSAPM is capable of the large-displacement, elasto-plastic analysis, and uses an out-of-core equation solver for efficient solution of large problems such as this one. The inelastic material behavior will be modeled with a bilinear stress-strain curve and both isotropic and kinematic hardening will be available for application. In the case of composite materials, a linear orthotropic material model is already available. If metal-matrix composites must be analyzed and anisotropic yielding is of concern, it appears that this effect can be accounted for with the use of Hill's theory of anisotropic yielding. Although not presently programmed in NOSAPM, the level of experience here indicates that it would not be overly difficult to accomplish. Centrifugal stiffening has been incorporated in NOSAPM through the addition of a body-force (centrifugal) load vector. This load vector is used to calculate centrifugal displacements which are used as initial conditions for the transient response. The constant centrifugal load vector is also added to the impact loads for each time step. The centrifugal displacements calculated by the initial state of the blade before the impact are also utilized in the calculation of eigenfrequencies and eigenmodes that indicate the effects of centrifugal stiffening.

If strain-rate effects are shown to be substantial in the course of material characterization, they will also be included. Flexible root fixity as well as blade interaction at the shrouds will be handled with spring elements. Figures 3(a) and (b) show the finite elements of the blade.

A successful compilation of the current version of the NOSAPM source file placed on the WPAFB CDC6600 computer system has been accomplished through the remote I/O site at Evendale. In addition, a successful check-out problem was run. This consisted of the flat plate shown in Figure 4, modeled with 20 noded elements, rotating at 5000 rpm and loaded with a transient load.

In order to facilitate the running of NOSAPM from Evendale, a data deck generator program is being written. This program is 90% complete and will generate card images of the NOSAPM input data based on element and node files (created with an existing mesh generator program available at Evendale) and on user input specified in the interactive time-sharing mode. The input data decks so created will be transmitted to the WPAFB 6600 systems via the remote Evendale I/O site to establish data files. Control of job execution in the batch mode is then accomplished at Evendale through time-sharing with the job output directed to the remote I/O site at Evendale.

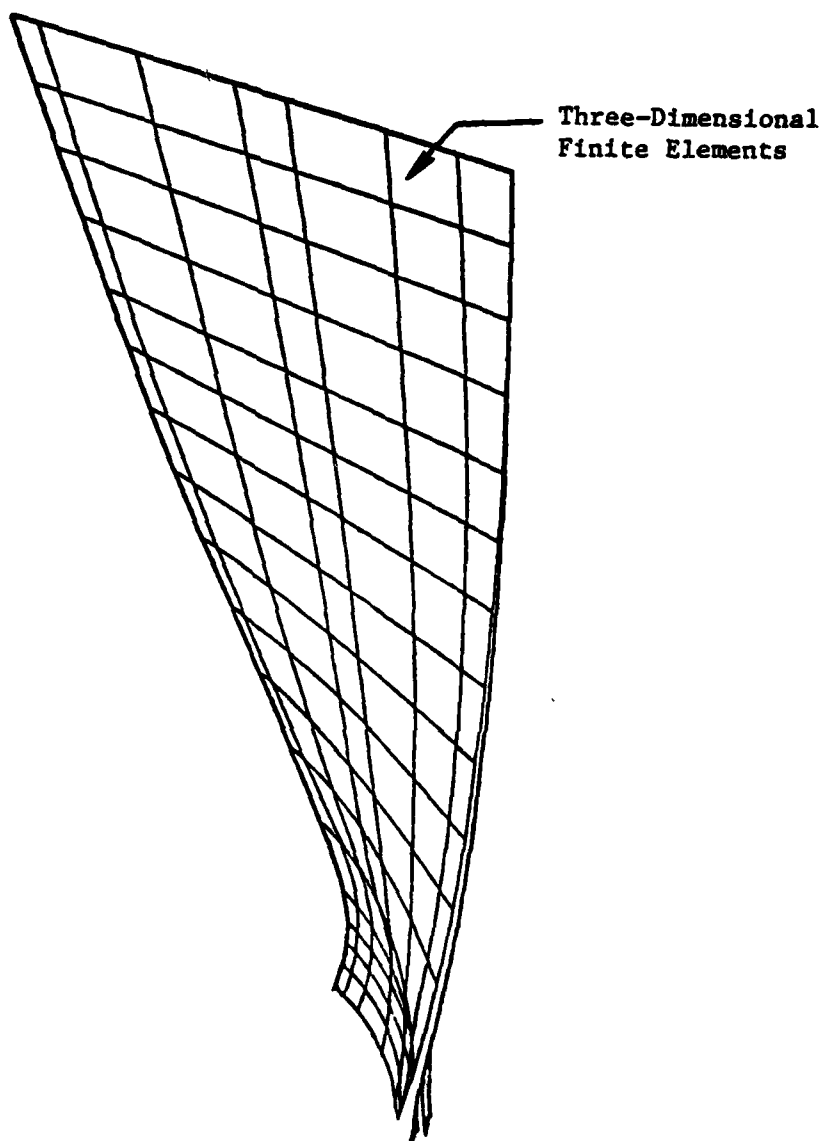


Figure 3(a). Level 1 Response Model Formulated
With 3-D Finite Elements.

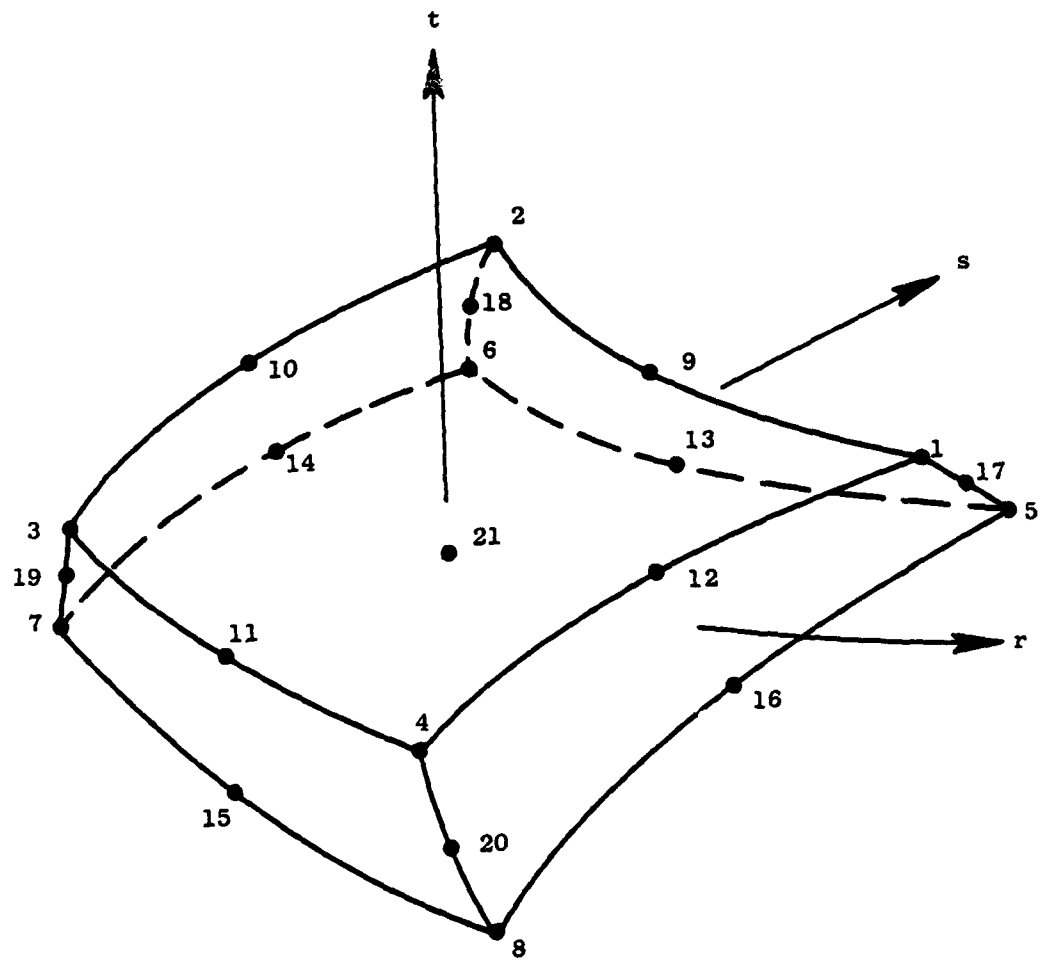


Figure 3-b. 3-D Finite Element Use in NOSAPM.

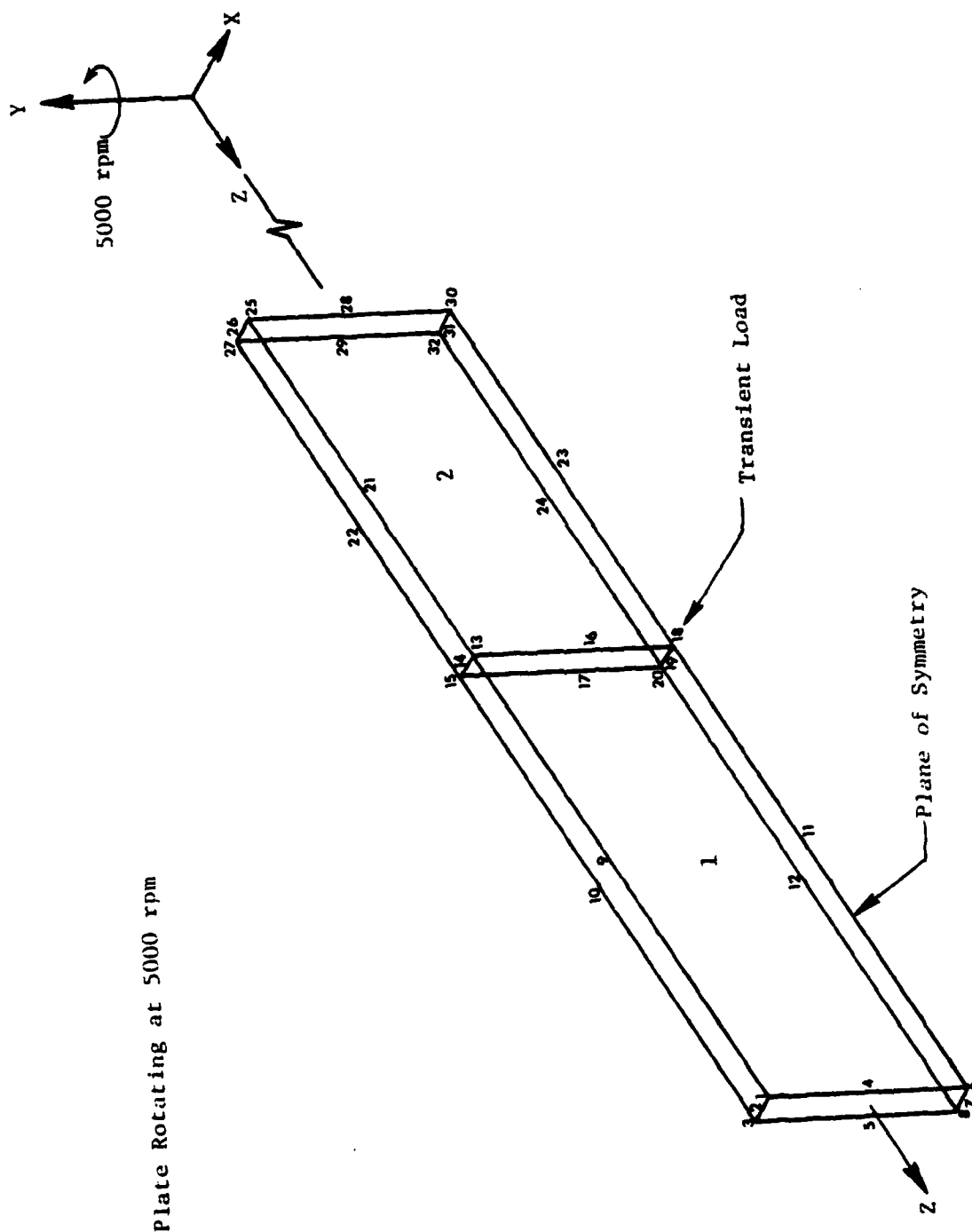


Figure 4. Plate Modeled for NUSAPM with 20-Noded Elements Rotating at 5000 RPM and loaded with a Transient Load.

4.3 SECOND-LEVEL RESPONSE MODEL (COMET-BLADE)

Essentially, the same physical effects are considered in the Level 2 (COMET-BLADE) analysis, but the elemental approach is somewhat simplified, thus contributing to gains in efficiency. The Level 2 analysis is based on the component element method³ and provides an analytical computer capability for predicting gross and local structural response of blades to representative large body impact loading stimuli.

Bending and membrane effects are modeled with a system of plate elements. These elements couple membrane and bending forces and are similar to those that have been highly successful in modeling both plasticity and hysteresis in the General Electric COMET-PIPE computer program⁴.

The formulation and programming of the plate elements for large deformations, material yielding and hysteresis effects are complete. These elements have nine nodes and address to three cases: (a) an element around a central node for interior regions of the blade; (b) a corner element; and (c) a middle-of-an-edge element. Figure 5 gives an indication of the Level 2 modeling.

The Level 2 analysis also includes centrifugal loading effects in a manner similar to that of the first level analysis and provides for the specification of damping that can be proportional to mass, to stiffness, or to a combination of the two. The blade can have twist and camber and can vary in thickness. Boundary conditions, such as restraint of rotation and displacement, can be specified.

The blade is modeled by giving the positions of nodes in global coordinates, the blade thickness, the material real-stress versus real-strain curve, the density, the damping, the speed in rpm, and the boundary conditions. The loads can be applied at any node in any direction. Step-by-step numerical integration is used to obtain a solution for the response. Still to be incorporated into the second level analysis is a material model that addresses to linear anisotropic effects and spring elements that allow for blade-to-blade coupling. This latter feature should be very useful in modeling the interaction of several blades due to the advantage of lower computing costs for the COMET analysis.

4.4 INTERFACE WITH THE LOADING MODEL

The interface between the response and loading models will be described in detail in the loading model section (Section 5). A brief description of the interface follows.

Since the impact loading due to the foreign object will depend upon the deformation of the blade, interaction between the structural model and the impactor model will be necessary. This requires the interfacing of the response routines developed by CR&D with the loading model developed by UDRI.

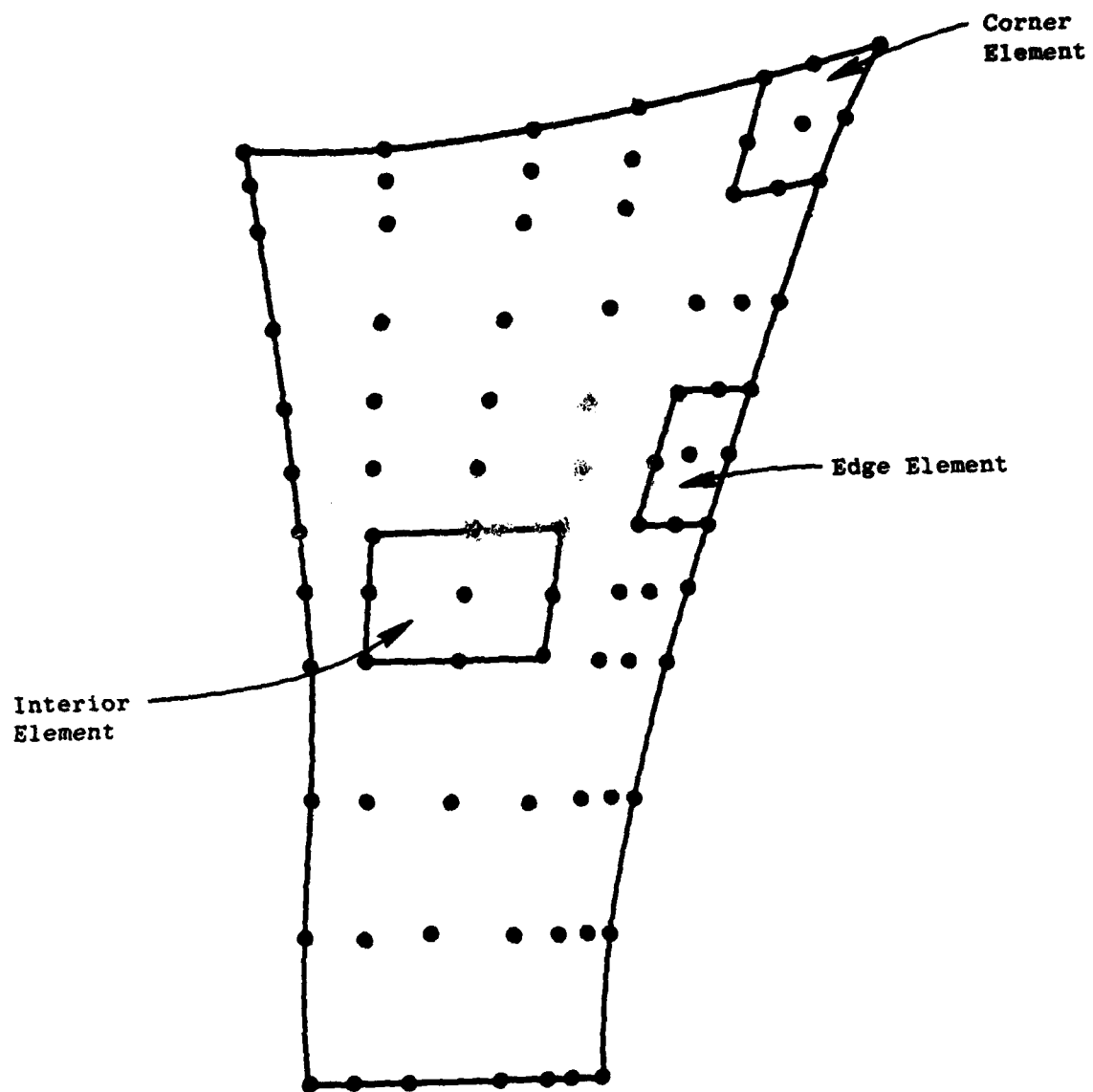


Figure 5. Level 2 Transient Response Model Formulated from a System of Plate Elements.

The interface between the first-level response model developed by CR&D and the loading model developed by UDRI has been accomplished. Geometric and dynamic information is periodically transferred from the structural analysis and used to update the impact loads. This need not be done at every structural time step of the transient analysis since large time steps may be suitable without loss of accuracy. The interface with the loading model will also be included in the second level response model. Figure 6 shows the linkup between the loading model subroutine and the executive or main response model program.

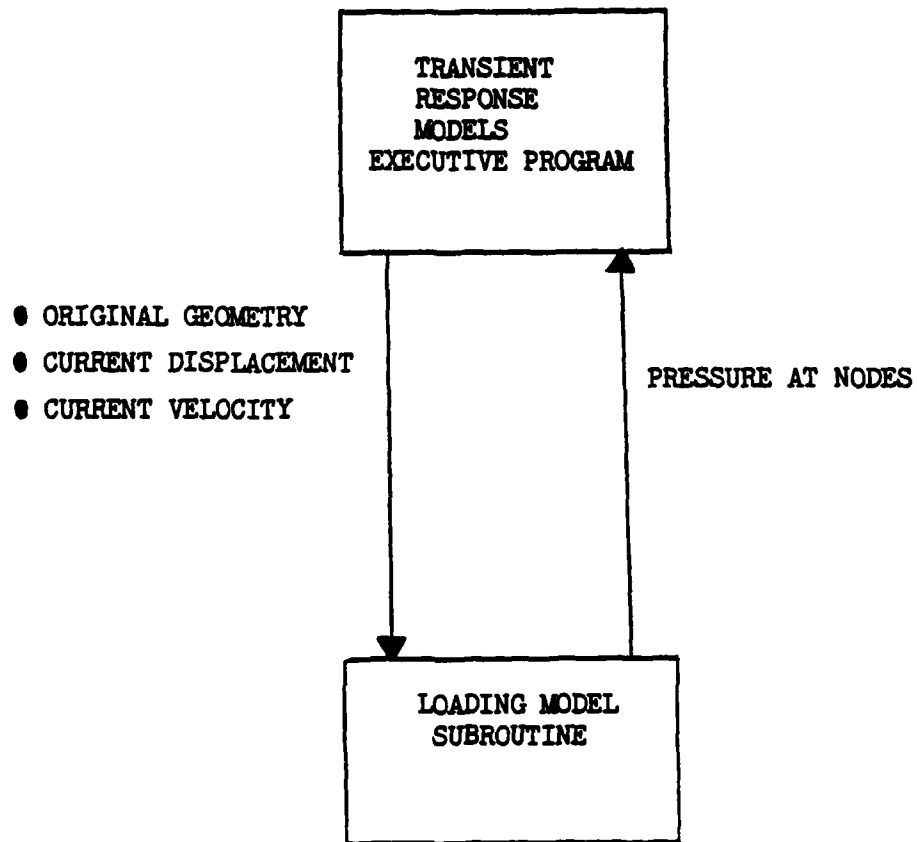


Figure 6. Link-up Between the Loading Model Subroutine and the Executive or Main Response Model Program.

5.0 TASK III - IMPACT LOADING MODEL

5.1 INTRODUCTION

The objective of this task is to generate an impact loading model for birds and ice which can be interfaced and used with the transient response structural analysis tools developed in Task II. The effort in this task is divided into four subtasks: (a) simulated bird and ice impact parameters; (b) loading model sensitivity study; (c) formulation/interfacing of loading model with structural models; and (d) experimental verification of loading model.

5.2 SUBTASK A - SIMULATED BIRD AND ICE IMPACT PARAMETERS

The work on this subtask has been completed. A report written by UDRI documenting the effort is currently being reviewed preparatory to transmittal to the Air Force. This report presents the results obtained from spatially and temporally resolved pressure measurements made during impacts of gelatin artificial birds and ice on rigid targets. Data are presented that show that gelatin behaves the same as real birds during impact and that the analytically predicted pressure distributions obtained with the loading model of Subtask C agree with the measured pressures for both bird and ice impacts.

5.3 SUBTASK B - LOADING MODEL SENSITIVITY STUDY

The purpose of the sensitivity study is to provide specific guidance as to which aspects of the loading model formulation must be modeled most accurately to properly predict specific aspects of blade response. The MARC/CDC finite-element code is being used for the numerical analysis in the sensitivity study. Nine, twenty-four and thirty-two 20-node brick element models were used to investigate the sensitivity of the response of typical blade-like structures to the details of impact loading. The 9- and 24-element models were used to predict the response of a flat cantilevered plate with the aspect ratio of the F101 first stage fan blade; Figure 7 shows the 9-element model. The results obtained with these 9- and 24-element models indicate that the momentum transferred to the plate is of primary importance. No significant local deformations were observed during loading with these models. The 32-element model was used to determine the importance of spatial and temporal loading on the local deformations of plate-like structures with nonconstant cross section. This model provided the relationship between loading (including the importance of initial high peak pressures) geometry, and mesh size on a detailed basis.

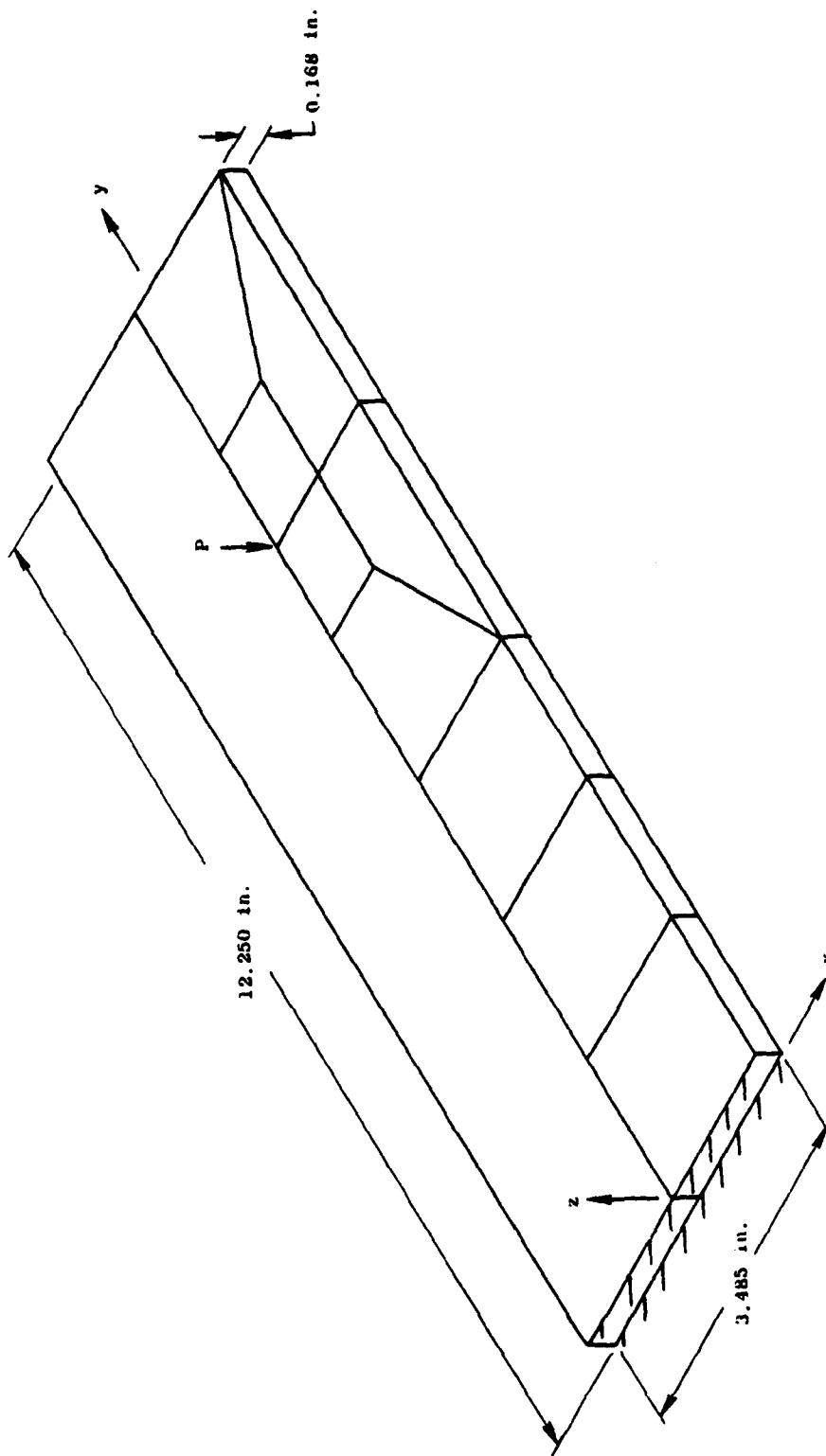


Figure 7. Loading Model Sensitivity Study, 9-Element 20-Node Brick Model of Cantilever plate Using Symmetry.

All of the required computer runs have been completed and the results have been factored into the formulation used for the loading model. A report summarizing the results is nearing completion.

5.4 SUBTASK C - FORMULATION/INTERFACING OF LOADING MODEL WITH STRUCTURAL MODELS

5.4.1 Introduction

The loads exerted on a structure during an impact can be characterized in terms of a number of fundamental parameters. The most important of these parameters is the total impulse imparted to the structure, the forces (i.e., the rate of impulse transfer), the pressures (i.e., the spatial distribution of the force), and the time variation of forces and pressures. The parameters that must be considered in a particular impact are a function of the response regimes of the target. We initially identified three response regimes and described suitable loading models for each regime. The Level 1 loading model was applicable to rigid, immovable targets. The Level 2 loading model was applicable to targets that translate and rotate but do not deform locally. The Level 3 loading model, the most general of the three, was applicable to impacts in which the target not only translates and rotates during impact, but also deforms locally.⁶

During the course of the present contract, we decided that only the Level 3 loading model was of major interest because of the response regime of fan blades and the relative ease of implementation. Subsequently, the original Level 3 loading model was renamed as the Level 1 loading model. Level 1 was thus used to denote both the most general loading model and the most general structural analysis model.

Described herein is the development of the Level 1 loading model for predicting the pressure distribution on a surface impacted by a bird or ice. The model is based on a fluid dynamic description of soft body impacts. Experimental evidence in the form of measured pressure distributions (spatial and temporal) during impact strongly supports the concept that bird and ice impacts are basically fluid dynamic in nature.⁶

The loading model developed specifically addresses the problem of birds, ice spheres, and slab ice impacting fan and compressor blades. The overall model consists of a model for the slicing of the impacting material by a row of blades and of a fluid dynamic model for describing the impact of an individual slice on a blade. The model is set up to interface with the structural analysis computer programs developed in Task II.

Described below are the slicing model, the fluid flow model of impact, the structure of the loading model subroutine, and the method used to interface the loading model subroutine with the structural response computer programs.

5.4.2 The Slicing Model

Because the forces required to slice a soft body are small compared to the forces required to decelerate the body, the slicing forces can be ignored. Therefore, the slicing model development reduces to simply a geometric problem of determining the dimensions and weight of a slice. For birds and ice spheres (such as hail), the velocity of the ingested object is small compared to the velocity of the aircraft; thus, the object velocity can be ignored. For slab ice, such as ice breaking loose from an engine nacelle, the velocity of the slab relative to the nacelle is not well defined; but we can expect that velocity is to be small in comparison to the aircraft velocity.

5.4.2.1 Slicing Model Development for Birds

The bird is idealized as a right circular cylinder with a length-to-diameter ratio of 2, and the velocity of the bird relative to the aircraft is taken to be equal and opposite to the aircraft velocity.

The bird/blade interaction geometry is shown in Figure 8. The given input data must include the number of blades per stage, the rotational speed of the blade (rpm), the radius from the rotational axis of the rotor to the point on the blade at which the center of the impact occurs, and the blade orientation angle.

An infinite number of slice shapes is possible for a given set of these input parameters; the shape depends on the orientation of the bird relative to the blade and on the span location on the blade at which the impact occurs. Since worst-case slice shapes are desired (i.e., slice shapes having the largest possible slice mass), the orientation of the axis of the bird and the center of impact of a slice were chosen to produce a slice having the largest possible mass. Figure 8 illustrates this orientation for a bird idealized as a right circular cylinder with a length-to-diameter ratio of 2. The largest slice mass occurs when the axis of the slice is coincident with the axis of the right circular cylinder. The bird slice mass is given by the following equation:

$$\text{Bird Slice Weight} = W_s =$$

$$= 2\rho D \left[h \sqrt{(D/2)^2 - (h/2)^2} + \frac{D^2}{2} \sin^{-1} \left(\frac{h}{D} \right) \right]$$

Where ρ = bird density = 0.91 g/cm³ (0.033047 lb_f/in³) and the other terms are defined in Tables 1 and/or 2.

The bird weight and the bird density together with the slice shape define the slice mass. The amount of bird slice consumed at any time during impact is directly related to the velocity of the bird relative to the blade (V_r in Figure 8) and the time from the beginning of impact.

Table 1. Blade Calculation Input Data Sheet For 3-Oz Bird.

Parameter	J79		APSI		F101
Rotor Speed, n (rpm)	7460		17500		7555
Number of Blades, N (-)	21		28		50
Tip Radius, R _t (in.)	14.65		11.00		22.18
Root Radius, R _r (in.)	5.21		4.95		11.71
Span Location (Z)	30	70	30	70	70
Radius, r _i (in.)	8.04	11.82	6.76	9.19	14.85
Orientation Angle, δ (°)	72.0	51.0	49.8	27.0	33.5
Chord Length, C (in.)	2.23	2.23	2.90	3.06	3.30
<u>Calculated Values</u>					
Blade Tangential Velocity, W _θ (ft/sec)	523	769	1032	1403	1255
Bird Axial Velocity, V _b (ft/sec)	200	200	200	200	200
Relative Velocity, V _r (ft/sec)	560	795	1051	1417	1270
Bird Weight, W _b (lb)	0.188	0.188	0.188	0.188	0.188
Bird Slice Width, h (in.)	0.86	0.89	0.29	0.29	0.37
Bird Slice Weight, W _s (lb)	0.126	0.129	0.045	0.045	0.057
Bird-Blade Incidence Angle, θ (°)	51.1	36.4	38.8	18.9	24.4
Angle β (°)	20.9	14.6	11.0	8.1	9.1
Bird Diameter, D (in.)	1.53	1.53	1.53	1.53	1.53

Table 2. Blade Calculation Input Data Sheet for 1.5-lb Bird.

Parameter	J79		APSI		F101	
Rotor Speed, n (rpm)	7460		17500		7555	
Number of Blades, N (-)	21		28		50	
Tip Radius, R _t (in.)	14.65		11.00		22.18	
Root Radius, R _r (in.)	5.21		4.95		11.71	
Span Location (Z)	30	70	30	70	30	70
Radius, r _i (in.)	8.04	11.82	6.76	9.19	14.85	19.04
Orientation Angle, ϕ (°)	72.0	51.0	49.8	27.0	52.5	33.5
Chord Length, C (in.)	2.23	2.23	2.90	3.06	3.30	3.70
<u>Calculated Values</u>						
Blade Tangential Velocity, W ₀ (ft/sec)	523	769	1032	1403	979	1255
Bird Axial Velocity, V _b (ft/sec)	200	200	200	200	200	200
Relative Velocity, V _r (ft/sec)	560	795	1051	1417	999	1270
Bird Weight, W _b (lb)	1.50	1.50	1.50	1.50	1.50	1.50
Bird Slice Width, h (in.)	0.86	0.89	0.29	0.29	0.37	0.38
Bird Slice Weight, W _s (lb)	0.53	0.55	0.18	0.18	0.23	0.24
Bird-Blade Incidence Angle, θ (°)	51.1	36.4	38.8	18.9	41.0	24.4
Angle β (°)	20.9	14.6	11.0	8.1	11.5	9.1
Bird Diameter, D (in.)	3.07	3.07	3.07	3.07	3.07	3.07

In addition to the idealized right circular cylinder slicing model for birds, slicing models will be also developed for ice balls and slab ice.

5.4.2.2 Slice Geometry Parametric Study

Bird slice parameters based on the right circular cylinder bird have been computed for both starling impacts (3-ounce weight) and larger bird impacts (1.5-pound weight). Three different blade configuration types (J79, APSI, and F101 engines) were considered; and typical values of the rotor speed, number of blades per stage, blade orientation angle, and impact radius were used.

Tables 1 and 2 show the input and computed parameters for the two bird size impacts. The primary observation from this parameter study is that these impacts are highly oblique (impact angles ranging from 51° down to 19°). The bird slice model has been incorporated into the loading model. For the loading model, the bird slice model essentially defines the velocity and shape of a fluid jet impacting a blade as well as the duration of the impact.

5.4.3 Fluid Flow Model of Impact

It has been demonstrated in Reference 6 that for birds having an L/D of 2 or greater the largest contributing factor in the total impulse of a bird impacting a target is the steady flow phase of an impact. Thus, in the current version of the loading model, the pressure distribution is based on a steady flow analysis. This method of analysis is extended into a dynamic analysis for deforming targets by treating the flow at any instant of time as a quasi-steady flow using the instantaneous relative velocity between the bird slice and the deforming target as the characteristic velocity. The instantaneous shape of target is used to define the surface on which impact occurs.

In the analysis of the impact process, the strength of the projectile material is considered to be negligible. This assumption is quite reasonable for the typical projectile and target materials of interest.

We assume that at least as a first approximation, the fluid flow may be treated as incompressible. This is a reasonable assumption because the measured steady-state pressures are quite small in comparison to the pressures required to produce significant density changes in birds or ice.

By virtue of the incompressible flow and steady flow assumptions and the negligible strength of the projectile material, the problem of predicting soft body impact loads is amenable to analysis within the following real constraints. The computing time required to obtain a reasonable solution must be small in comparison to the computing time required to compute the structural response, and the computer storage requirement for the loading model must be small in comparison to the structural response analysis computer program storage requirements.

Three-dimensional potential flow theory was chosen as the most appropriate method for modeling the impact process. Our initial work in using this approach was quite successful.⁷ In that work, we used the method of surface singularities to determine the velocity and pressure fields caused by circular jets impacting at oblique angles on flat rigid plates. This same technique was used to develop the loading model. The method developed earlier was generalized to include the impact surface curvature and deformation velocity, an arbitrary cross-sectional area of the impacting flow, and a method for generating planar quadrilateral surface elements from given finite-element surface nodal point locations.

5.4.3.1 Surface Singularity Method - Superposition of Onset Flow and Surface Source Distribution

The impacting bird slice is idealized as an onset flow of velocity, V_r , uniformly distributed over the cross-sectional area of the slice. The fluid velocity at a point is expressed as the negative gradient of a potential function that satisfies Laplace's Equation in the region exterior to the blade, that has a zero normal derivative on the blade surface, and that approaches the proper uniform stream potential function. The flow is viewed as an onset flow potential and disturbance potential due to the blade. The disturbance potential satisfies the Laplace's Equation in the exterior and the appropriate normal derivative condition on the surface and vanishes at infinity. From potential theory, it can be shown that this potential may be evaluated in terms of a surface source density distribution with which the blade surface may be considered to be covered. The incorporation of the normal derivative condition on the surface produces a source density distribution described by a two-dimensional Fredholm Integral Equation of the second kind over the surface. Once this equation is solved for the source density distribution, first the disturbance potential and then the disturbance flow velocities may be obtained.

5.4.3.2 The Body Surface Approximation

In the numerical solution of the Fredholm Integral Equation for the surface source density distribution, the body surface must be suitably approximated. The body surface is approximated by a large number of small plane elements that are formed from the original points defining the body surface. The calculations employ plane quadrilateral elements, and the source density is assumed constant over each of these elements. With this assumption, the problem of determining the continuous function for the source density reduces to one of determining a finite number of values - one for each of the planar elements.

5.4.3.3 Solution Procedure

This section presents a brief description of the method of solution.

As a first step, it is necessary to prescribe the input points, a set of points in three-dimensional space describing the body surface. These input points should be chosen to provide the best representation of the body with the fewest possible points. Four of these inputs are employed to generate one plane quadrilateral source element of the body surface.

Once the values of the surface source density have been determined, the velocity components at each null point are calculated; and the appropriate components of the onset flow are added. The resultant velocities and pressures are easily computed from the velocity components.

5.4.3.4 Onset Flow Modeling

When it is used with the surface singularity technique, the simple onset flow model described in Section 5.4.3.1 is adequate for normal impacts and also for oblique impacts, provided that the angle of incidence (the angle θ in Figure 8) is greater than about 30° . For small values of θ , a more sophisticated onset flow model is used. The basis for this more accurate onset flow model is a two-dimensional jet flow theory for oblique impacts.

5.4.4 Structure of the Loading Model and Interface With Response Models

We have incorporated in our analysis a procedure for finite-difference numerical computation of the potential flow about arbitrary three-dimensional bodies that has certain features that render it compatible with the finite-element structural response analysis code. Specifically, the nodal points in the finite-element program become approximate locations of the null point (defined to be the point where the quadrilateral element induces no velocity in its own plane) around which the plane quadrilateral elements are constructed in the potential flow analysis. This greatly facilitates the coupling of the finite-difference loading model and the finite-element structural code.

In loading used for any arbitrarily shaped impact surface, the impact area is divided into small flat elements; and a uniform distribution of sources is assumed to cover each area. At the beginning of impact, an initial pressure distribution is computed for the undeformed blade. During an impact in which local deformation takes place, the deformed shape of the impact zone is calculated in the dynamic structural response analysis. After significant deformation has occurred, the geometry of the impact zone is provided to the loading model. The loading model is then used to calculate a new pressure distribution. As the structural analysis calculation proceeds, the local shape, the location, and the velocity of the impact area are updated and passed to the loading model at appropriate time intervals. The loading model, in turn, provides updated pressure distribution information for the structural response computation. The loading model is fully interactive with the structural response calculation. The duration of the impact is computed by keeping track of how much slice has been consumed during each time interval.

A summary of the interface between the loading and response models follows:

- The response model provides displacements and velocities at the surface nodes of the structural elements in the impact region. These structural elements are then subdivided into smaller elements corresponding to the finer grid of the loading model as specified by user input, and the structural element shape functions are then used to compute the displacements and velocities at the nodes of the smaller elements. These displacements and velocities are provided to the loading model at specified time steps.
- The slice size calculations are based on user input and are performed by the response program. The impactors that will be available to the user include the following:
 - Bird of any weight represented by a right circular cylinder having L/D ratio equal to 2.0.
 - Ice ball of any diameter.
 - Slab ice of any thickness and length.

User-provided information (in addition to the geometry and material properties of the finite element response model) will consist of the velocity of the aircraft, the rotational velocity of the fan or compressor, the number of blades in the stage, the spanwise location of the impact, and the specification of the impactor.

- The loading model provides the pressures at the nodes of the smaller elements, and the structural element shape functions are then used to calculate the pressures at the nodal points of the structural elements. These pressures are then converted to equivalent nodal focus through a consistent force formation.
- A flag is returned by the loads model when the impactor has been consumed (i.e., when it has traveled its own length). When this occurs, the response model will no longer call the loading model subroutine and the nodal pressures are set to zero.

The loading model is capable of detailed interaction with the structural response model and of dealing with target translation, rotation, and local deformation. The load/response coupling modeled in this formulation should be capable of accurately predicting both overall target response and local deformation.

The principal limitation of the loading model is that it does not include transient effects. The most significant transient effect is the shock effect; however, the porosity present in birds appreciably reduces the shock stresses without significantly affecting steady flow pressures. In addition, impact

obliquity reduces the relative importance of shock stresses. Therefore, it is not obvious that neglect of the shock aspects of bird impact on blades is a significant deficiency. Another transient aspect of bird impacts is the variation of slice cross section at the target surface during impact. This variation results mainly in a time variation of the impact area. If the flow remains quasi-steady during these variations (i.e., the "velocity" of the variation is low with respect to local sound speed - probably a good assumption), then the loading model can be modified to described these effects. The size and geometry of the "jet" that flows onto the target surface must be updated incrementally to describe the variation with time of the impact area.

5.4.5 Summary

A loading model has been developed for soft body impacts on structures that respond to the impact in a very general manner. The loading model was developed from a fluid dynamic description of a soft body impacting (flowing onto) a structure. The structure can translate, rotate, and deform locally during the impact. The model is based on an approximate solution to the problem of the quasi-steady flow of a jet of arbitrary cross section flowing onto a surface with an arbitrary shape.

The cross-sectional area of the jet is determined from an analysis of the slicing of soft bodies by a row of fan or compressor blades. The loading model pressure distributions show excellent agreement with pressure distributions obtained in experiments in which birds, substitute birds, and ice spheres impacted on rigid targets. The loading model has been successfully interfaced with the first level finite element structural analysis computer program.

The overall validity and limitations of the model will be determined by comparing the structural response predicted by the combined loading model/structural analysis model with that observed in experiments.

5.5 SUBTASK D - EXPERIMENTAL VERIFICATION OF LOADING MODEL

In order to check the adequacy of the integrated loading and response models, comparisons will be made between the analysis predictions and the test results for impacts on cantilevered plates. A range of impact parameters (mass for substitute birds and ice, velocity and incidence) will be employed to ensure a full range of specimen response modes (i.e., elastic, elastic-plastic structural deformation, and severe local deformation). The predictions of the complete model will be compared to experimentally derived results obtained from Task VI - Structural Element tests. For some of cantilever plate tests of Task VI, a Moire fringe technique will be used to obtain displacements. We will, therefore, accomplish the objectives of both Task III-D and VI with one set of experiments.

Once the selected structural element impact tests are accomplished, a detailed comparison between the experimental and analytic results will be made and the source of any discrepancies will be identified. Any modifications required in the loading model which are identified in this subtask will be made.

6.0 TASK IV - MATERIAL RESPONSE AND FAILURE CRITERIA

6.1 SUBTASK A - GROSS STRUCTURAL DAMAGE PROPERTIES

6.1.1 Introduction

Testing is proceeding along two fronts in order to establish gross structural material response and failure data. First, bench impact tests have been conducted using the full-scale blades selected in Task V. The strain rates pertinent to the problem of foreign object impacts have been determined from these tests. Impact tests, using the parameters of Tables 1 and 2, have been conducted on three different type blades, two of which are unshrouded. The two unshrouded blades are the stainless steel J79 first stage compressor blade and the B/Al composite APSI first stage fan blade. These blades were cantilever-mounted at the root. The third blade type is the titanium F101 first stage fan blade. This blade is tip shrouded and, therefore, was fastened at both ends. Each blade type was impacted at the 30 and 70% span locations and two blades of each blade type were used.

In the second part of Subtask A, tests are being conducted to obtain material property data for the relevant strain rates. Forged bar stock was used to make the metal specimens (8Al-1Mo-1V titanium to represent the F101 blade, and 410 stainless steel to represent the J79 blade). The 410 is being substituted for the 403 which is unavailable. Chemically, the two alloys are the same except for a small amount of chromium, an element which does not affect the room temperature mechanical properties. Standard cylindrical specimens are used for the tension tests at low and intermediate strain rates and the entire stress-strain curve is obtained using strain gages and an extensometer. The change in diameter is used to calculate Poisson's ratio. The high strain rate tests are conducted on the split-Hopkinson bar using the standard tension test specimen for that apparatus. All of the metal specimens have been designed and fabricated.

The advanced composite selected for the study is boron/aluminum used in the APSI Stage 1 fan blade with a fiber layup of (0/22/0/-22). The 4-mil boron fibers are in a matrix of 2024 aluminum. Each ply is 4.7 mils thick and does not, in general, run the length of the blade. The center ply of the blade is a plate of aluminum. On either side of it is a ply of stainless steel wire mesh. The next plies on both sides are the B/Al layup. The entire outer blade surface is covered with a ply of stainless steel wire mesh. The leading edge has a thin coat of pure nickel.

The material properties are needed in three principal directions because the composite is anisotropic. The data needed are the tensile stress-strain curves for each direction, three Poisson's ratios, and three shear stress-strain curves. However, the collection of this information is simplified considerably by the use of laminate theory. This theory employs the results of material property tests on unidirectional specimens to calculate the bulk properties of the angle-ply layup.

The composite test specimens have been designed and fabricated and the experimental methods that will be employed to obtain the composite material properties have been established.

6.1.2 Real Blade Strain Rates

Testing of the full-scale blades to obtain the maximum strain rates has been completed. The highest strain rates developed were less than 400 in./in./sec in any of the types of blades tested (J79, F101, and APSI). For the J79 impacts, the highest strain rate for the 30% span impact was 344 in./in./sec for a 1.5-pound bird impact. This value was for a gage located on the midchord at the root in the spanwise direction. For the 70% span impact of the J79 blade, the highest strain rate was 362 in./in./sec which was for a 1.5-pound bird impact. This value was for a gage directly behind the impact site which was oriented in the chordwise direction.

The highest strain rate for the 30% span impacts of the tip restrained F101 blade was 341 in./in./sec. For the 70% span impacts of this blade, the highest strain rate was 367 in./in./sec. Both strain rates were for 1.5-pound bird impacts and for a gage location at the tip along the leading edge in the spanwise direction.

For the APSI blade, the highest strain rate developed was 366 in./in./sec for a 70% span impact of a 3-ounce bird. This occurred at a gage location at the midchord of the root in the spanwise direction. The highest strain rate for the 30% span impact was 362 in./in./sec for a 3-ounce bird. This gage location was behind the impact site with the orientation of the gage being in the direction of the chord.

Figure 9 shows the impact test setup used for real blades. Shown in this figure is the cantilever mounted J79 blade. The slicer and the target blade are oriented relative to the path of the projectile to provide the slice weight as defined in Tables 1 and 2. For example, to simulate the impact on the J79 blade for a rotor speed of 7460 rpm (maximum engine speed) and a bird velocity of 200 ft/sec, bird-blade incidence angles and impactor velocities of 51.1° and 560 ft/sec and 36.4° and 795 ft/sec are required for 30% and 70% span impact locations, respectively. For a 3-ounce bird, the 30% and 70% span impact parameters result in slice weights of 0.126 lb and 0.129 lb, respectively.

Figure 10 shows the strain gage locations used to determine the strain rates for the J79 blade. Figures 11 and 12 show examples of the J79 blade response resulting from simulated bird impact. Shown in these figures are the measured strain-time and computed strain rate-time histories for Gages 1 and 3 for a 3-ounce bird impact on the J79 blade. Figure 13 shows the strain in both the time and frequency domains resulting from a hammer blow.

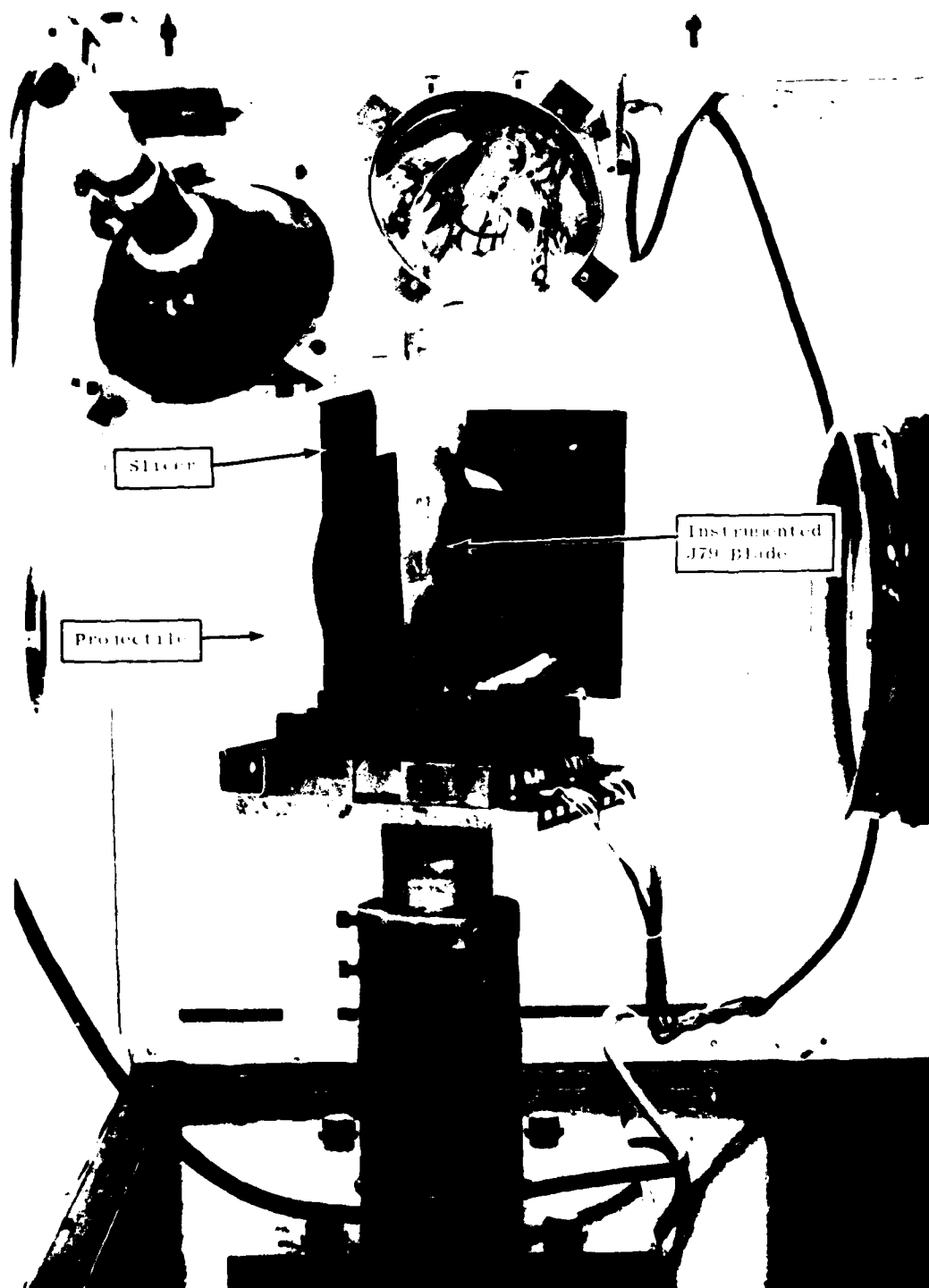


Figure 9. Bench Impact Test Setup for Real Blades

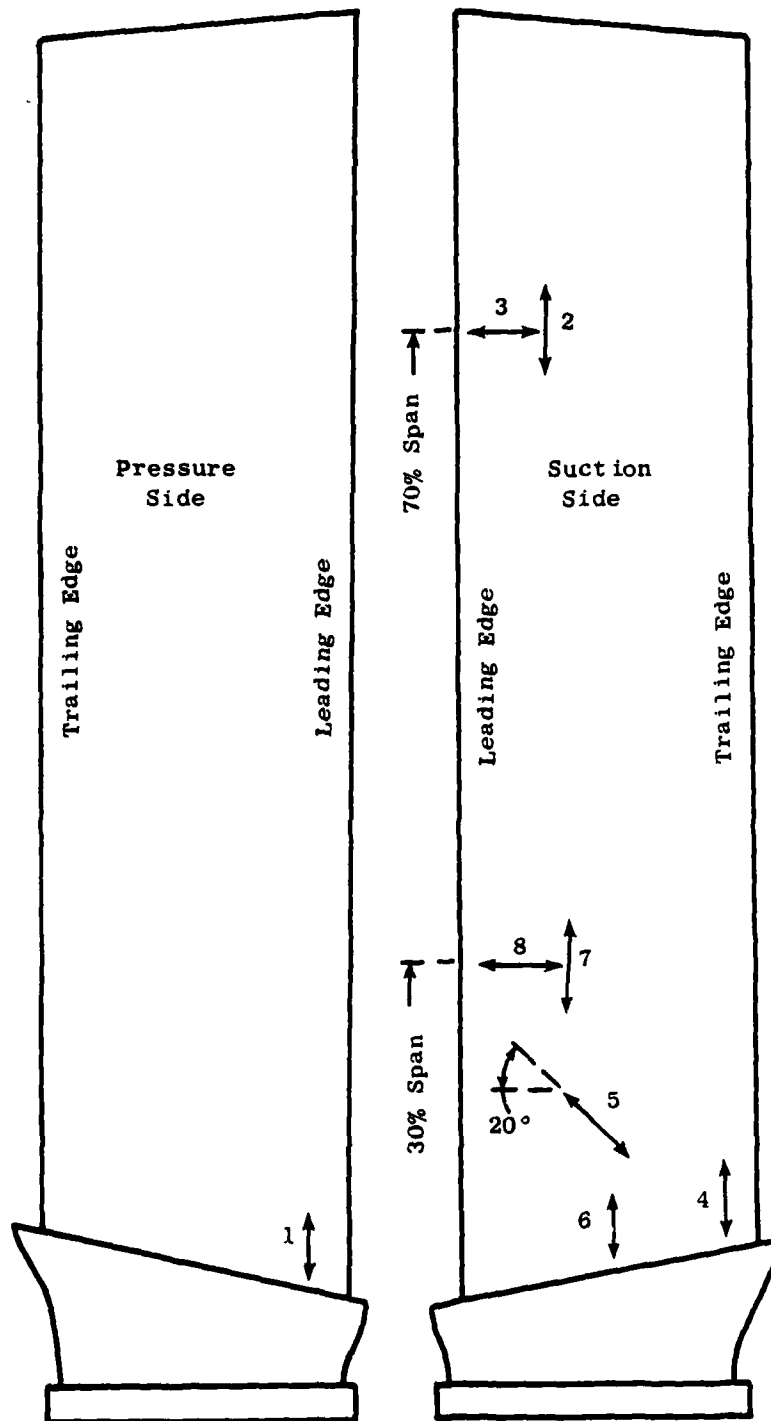


Figure 10. J79 Stage 1 Compressor Blade Strain Gage Locations for Maximum Strain Rate Determination.

3 OZ. BIRD IMPACT ON J79 BLADE AT 70% SPAN
TEST DATE 10-16-78
SHOT 2-0021

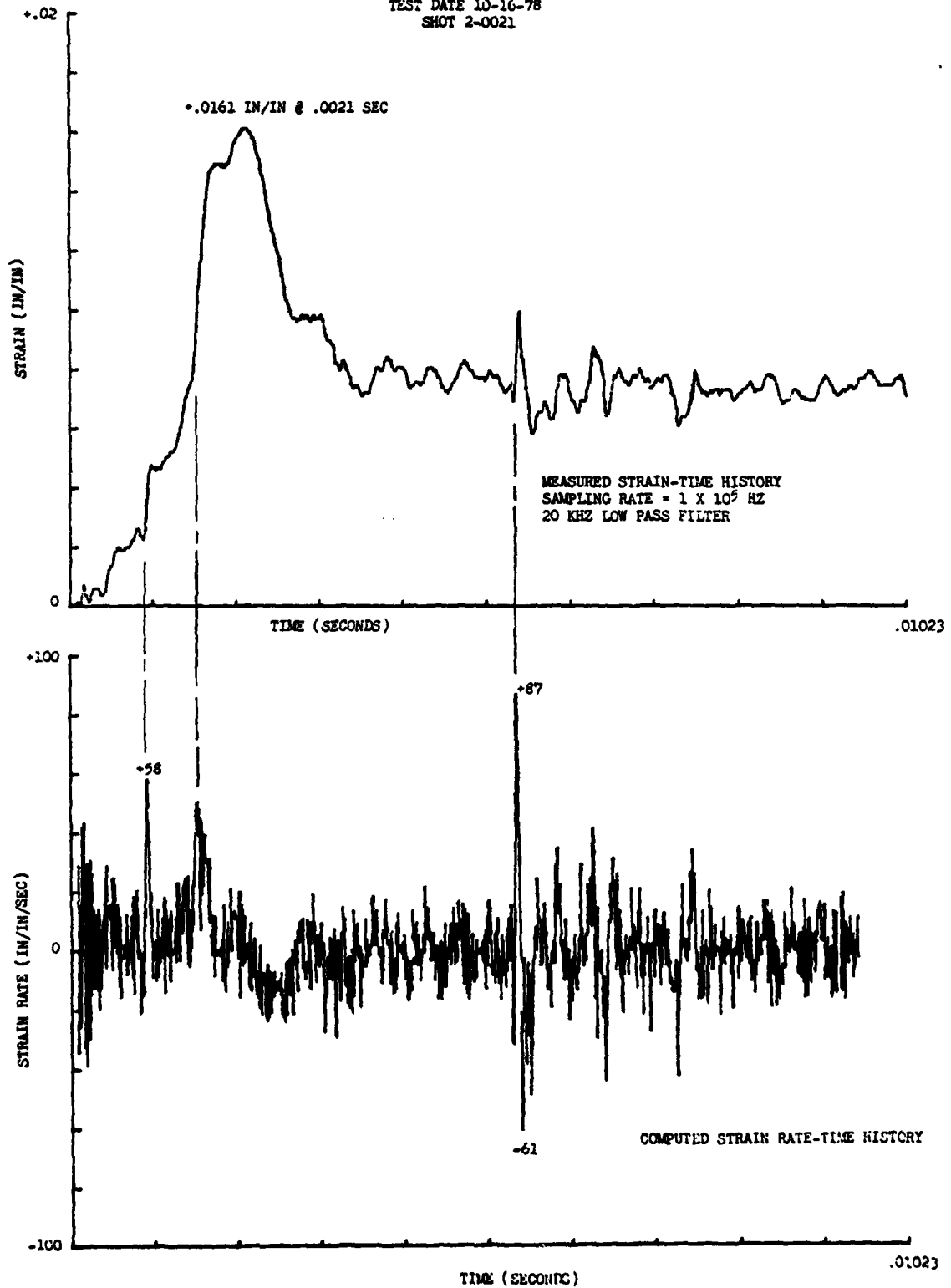


Figure 11. Strain and Strain Rate Time Histories for Gage No. 1
(at Root of Airfoil on Pressure Side).

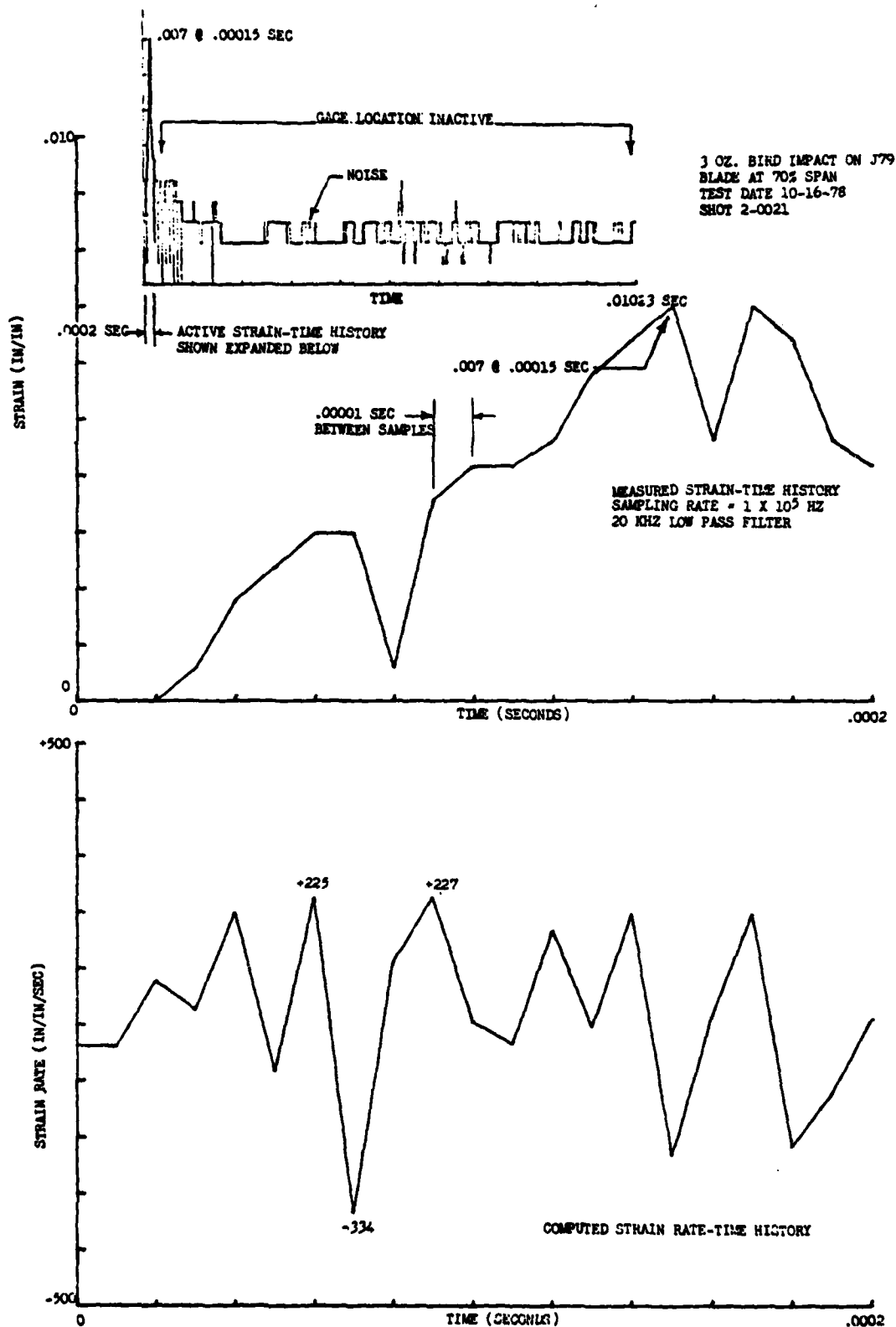


Figure 12. Strain and Strain Rate Time Histories for Gage No. 3.

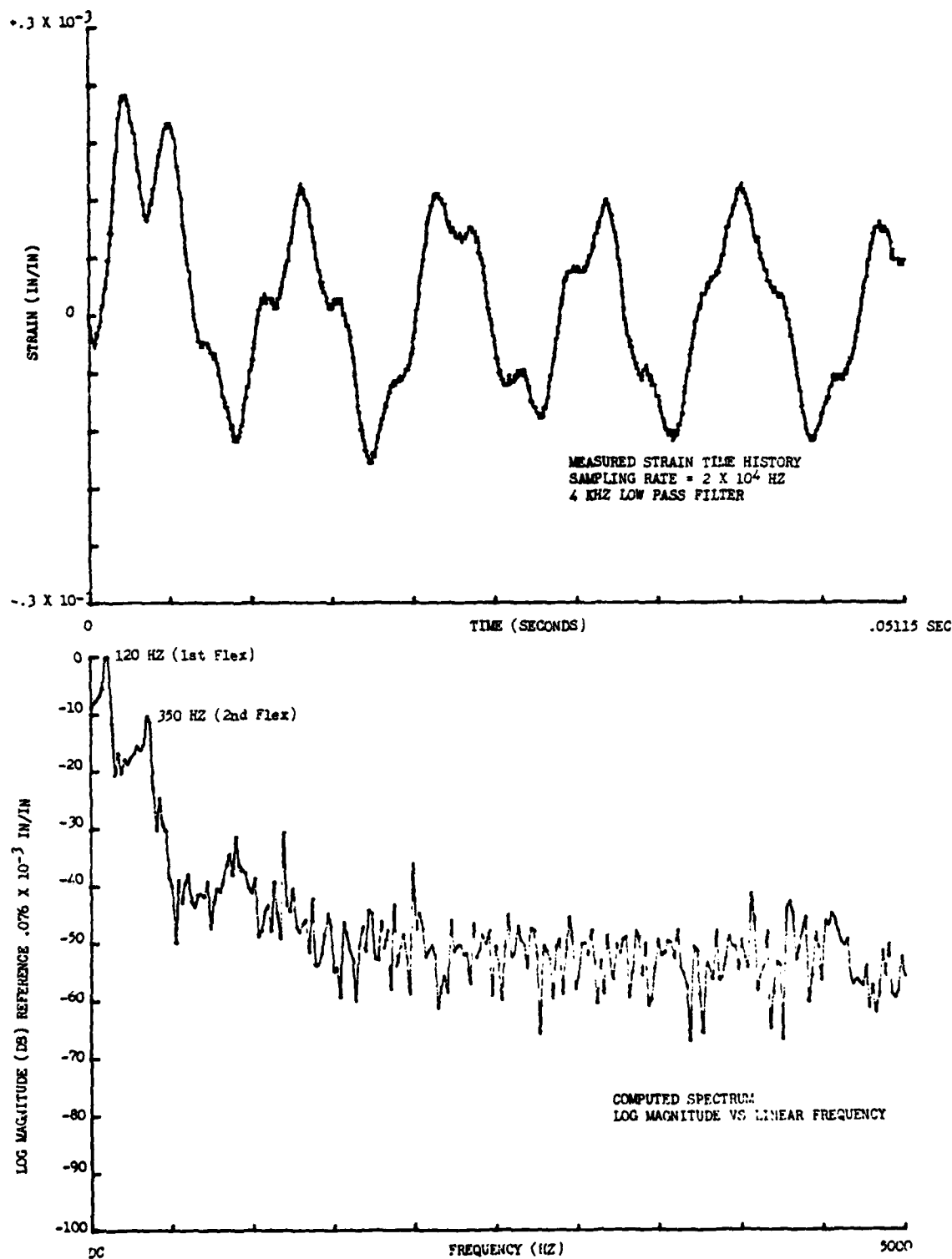


Figure 13. Strain in the Time and Frequency Domain Resulting from Hammer Blow for Gage No. 4 J79 Blade, Test Date 10/16/78.

The bird impact response data shown in Figures 11 and 12 correspond to plastic response behavior in the blade. This blade experienced yielding at both the root and the impact site as a result of the impact. In this case, the actual impact velocity was 984 ft/sec and not 795 ft/sec and the actual slice weight was 0.0619 lb (28 gms) and not 0.129 lb (58.5 gms) as specified in Table 1. In addition, the substitute bird impacted the blade somewhat above the 70% span location. The strain rates were computed from the measured strain-time history by employing Fourier transform techniques. This was accomplished by using the duality between the derivative of a time function and the complex product formed from the Fourier transform of the time function and the factor $(j\omega)^n$; j is the imaginary direction in the complex plane, ω rad/sec is the frequency and n is the order of the derivative. This approach is expressed mathematically in the development shown below.

The Fourier transform of the original time function (strain-time history) $X(t)$ is equal to

$$X(\omega) = \int_{-\infty}^{\infty} X(t) e^{-j\omega t} dt$$

The Fourier transform $X_D(\omega)$ of the first derivative (strain rate) $\dot{X}(t)$ can be obtained from the Fourier transform of the original time function $X(t)$ as follows:

$$X_D(\omega) = \int_{-\infty}^{\infty} \dot{X}(t) e^{-j\omega t} dt = j\omega X(\omega)$$

Finally, the strain rate, $\dot{X}(t)$, is obtained via the inverse Fourier transform.

$$\begin{aligned} \dot{X}(t) &= \int_{-\infty}^{\infty} X_D(\omega) e^{j\omega t} d\omega = \\ &= F^{-1} \left[j\omega X(\omega) \right] \end{aligned}$$

The spectrum shown in Figure 13 corresponds to the elastic response behavior obtained with the hammer blow. Two dominant response peaks are in evidence at 120 Hz and 350 Hz. These frequencies correspond to the bench test frequencies for the first and second flex modes of the cantilever-mounted J79 blade.

6.1.3 Material Property Data

The material characterization tests on the two metals, 410 stainless steel (410 substituted for 403) used for the J79 Stage 1 compressor blade and titanium 8Al-1Mo-1V used in the F101 Stage 1 fan blade, are currently underway. The tests on the advanced composite (B/Al) used in the APSI Stage 1 fan blade have not yet started. As mentioned previously, the advanced composite used in the APSI blade is actually a hybrid composite. This blade has the following layup: SSWM/0°/22°/0°/-22°/SSWM/Al/SSWM/-22°/0°/22°/0°/SSWM. It will, therefore, be necessary to characterize the stainless steel wire mesh also.

The strain rates for the metals tests are shown in Table 3. The upper limit is that value determined by the real blade impact testing.

Table 3. Characterization of Metallic Materials.

<u>Material</u>	<u>Strain Rates (sec⁻¹)</u>
410 Stainless Steel	0.001, 0.1, 1, 10, 100, Highest
8Al-1Mo-1V Titanium	0.1, 10, Highest

The metal tests at the lower strain rates, 0.001 e/sec, 0.1 e/sec, and 1.0 e/sec, have been conducted. In addition, the high strain rate material properties tests using the split Hopkinson bar apparatus have also been conducted. The strain rates for these high strain rate tests varied from 530 to 570 e/sec for the 8-1-1 titanium, and 340 to 760 e/sec for the stainless steel (the larger range in strain rates on the stainless steel was achieved by setting the striker bar to attain different velocities). The maximum rates are higher than the impact tests on the blades indicated were necessary. The data have been digitized and graphed. The metal tests at 10 e/sec and 100 e/sec have not yet been accomplished. The low and intermediate strain rate tests (0.001-10 e/sec) have been conducted per standard ASTM E8-69⁷ and the specimen definition is shown in Figure 14. The standard tensile specimen used for the high strain rate tests on the split Hopkinson bar is shown in Figure 15.

The test matrix that will be used for the characterization of the boron-aluminum and the stainless steel wire mesh is shown in Table 4. For the tensile tests in the direction of the symmetry axes (0° and 90°), a modified ITTRI specimen configuration will be used.⁸ This specimen is shown in Figure 16. For the shear tests in the interlaminar plane, the 10° off-axis shear test developed by Chamis and Sinclair⁹ will be used for the B/Al. A drawing of the specimen appears in Figure 17. Torsion rod specimens will be used to

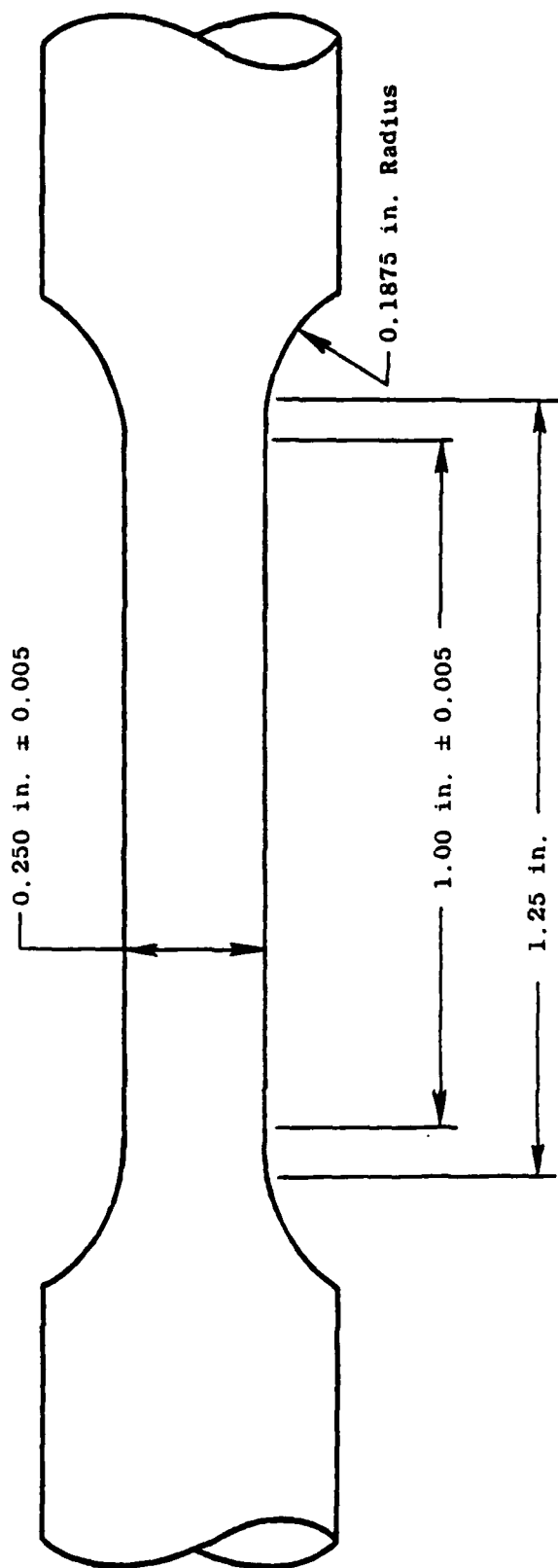


Figure 14. Tensile Specimen for Metals.

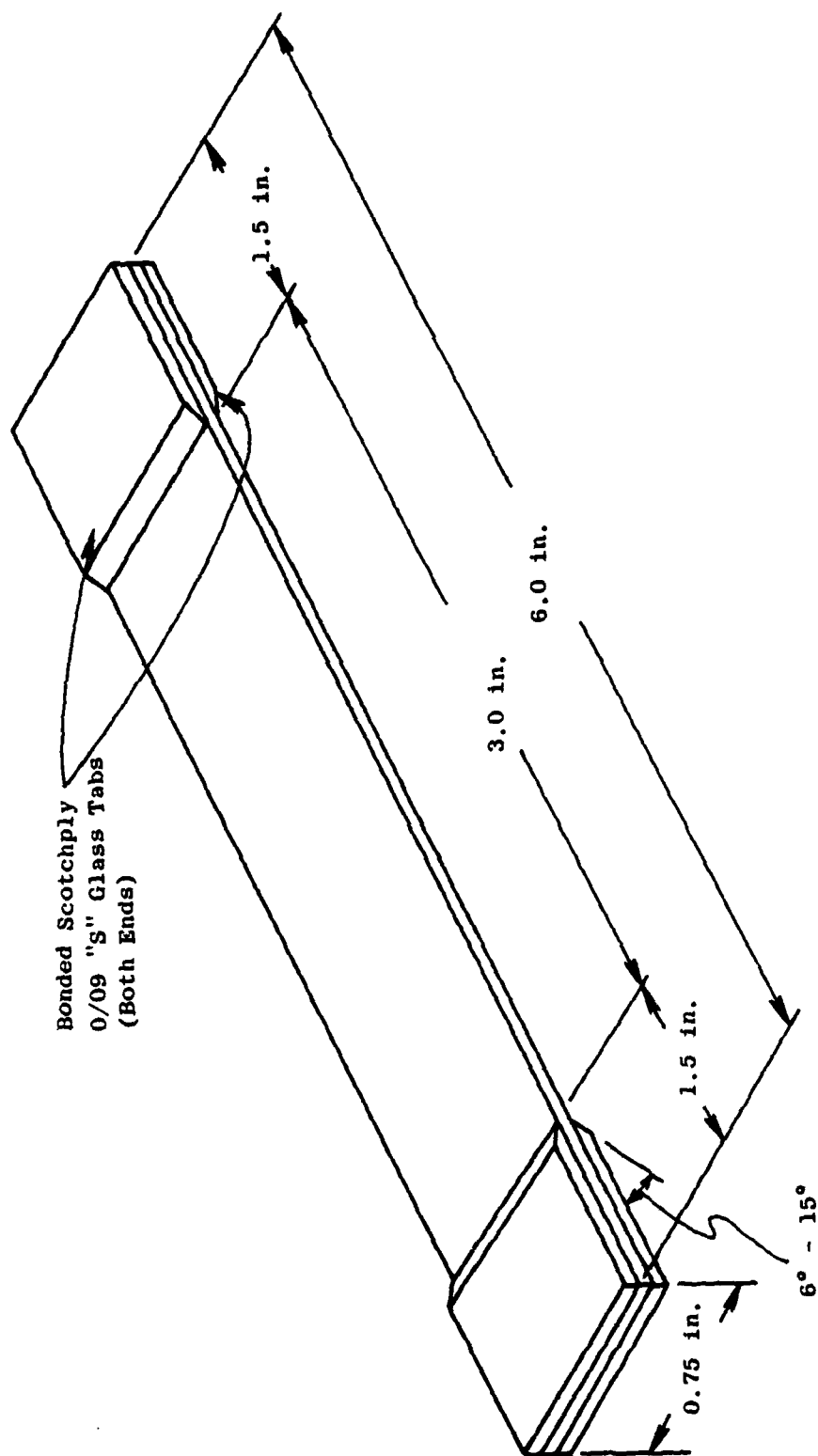


Figure 16. Modified ITTRI Specimen.

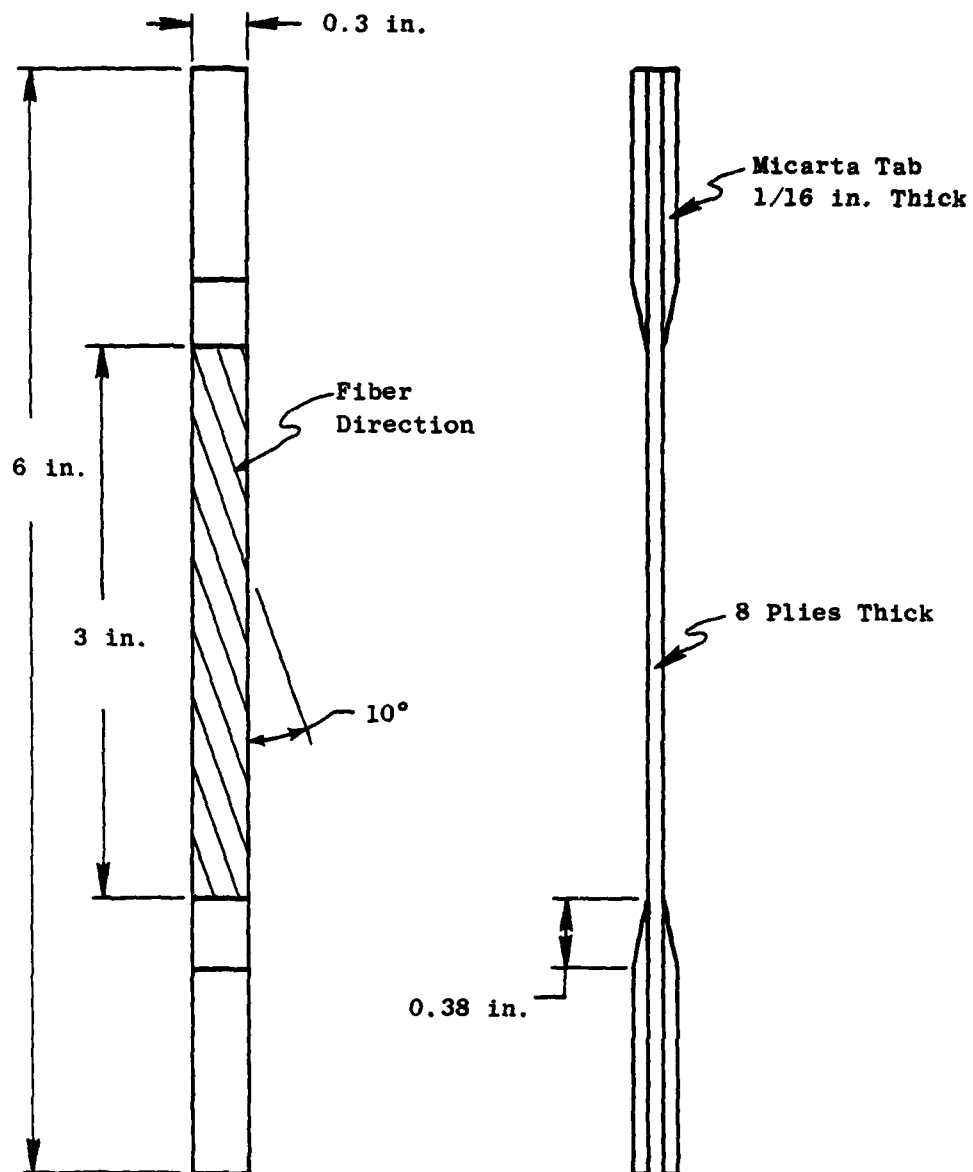


Figure 17. Modified 10° Off-Axis Shear Specimen.

determine the transverse shear properties for both the B/Al and the stainless steel wire mesh. The in-plane shear properties for the stainless steel wire mesh will be determined with the $\pm 45^\circ$ shear panel specimen.

Table 4. Characterization Tests for B/Al and Stainless Steel Wire Mesh.

<u>Material</u>	<u>Test Description</u>	<u>Strain Rates (sec⁻¹)</u>
B/Al	0° Tension	1,10
	90° Tension	1,10
	10° Off-axis Shear	10
	Rod Torsion Shear	10
SSWM	Tension (in plane)	1,10
	Torsion (through the thickness)	1,10
	$\pm 45^\circ$ Shear	10
	Rod Torsion Shear	10

The through-the-thickness tensile specimen shown in Figure 18 will be used to determine the normal to the plane tensile properties for the stainless steel wire mesh. The tensile specimens (include 10° off-axis and $\pm 45^\circ$ panels) will be instrumented with high resistance strain gages. For the through-the-thickness and torsion rod specimens, it is planned to use an extensometer to measure displacement.

It is not anticipated that the composite will be significantly strain rate sensitive. Strain rate effects in B/Al were investigated by Krinke, Barber, and Nicholas¹⁰ using a three-point bend (Charpy impact) technique. They found no significant strain rate effects over 6 orders of magnitude; the highest strain rate employed in the study was 100 sec⁻¹.

6.2 SUBTASK B - LOCAL LEADING EDGE DAMAGE

6.2.1 Introduction

This subtask is concerned with the generation of empirical design data for local leading edge damage to first stage fan and compressor blades. Testing is being conducted to determine and quantify the damage caused by leading edge impacts for a range of pertinent impact conditions. The results of this study will include data expressed in terms of the residual properties of the materials which are directly relevant to fan and compressor designers.

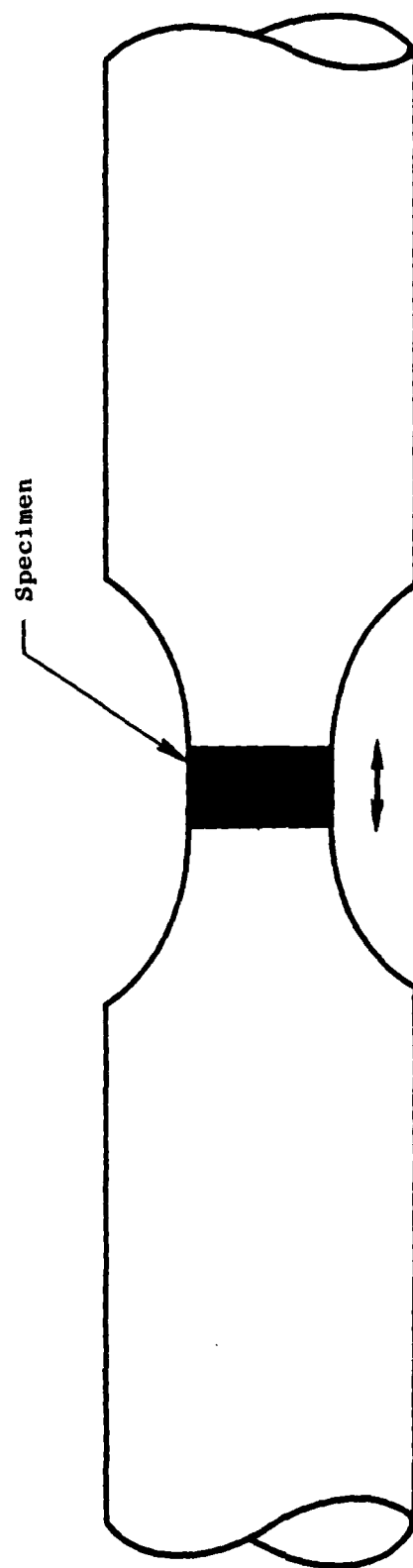


Figure 18. Through-the-Thickness Test Specimen.

6.2.2 Overall Approach

Three types of blade materials, geometries, and sizes will be investigated using substitute bird materials, ice, granite pebbles and steel spheres as the impactors. This range of impactors is representative of the types of objects commonly ingested into engines. The three blade types are the J79 blade using type 403 stainless steel, the F101 blade using 8-1-1 titanium, and the APSI metal matrix boron/aluminum blade. Fabricated metal and composite specimens and actual APSI blades will be tested. The geometries of the leading edges of the fabricated specimens will be similar to the geometries of the blade types at the 50% span location. Three specific investigations are planned in this subtask. The first establishes a base of damage data. The second addresses scaling and subscale tests, while the third investigates the effects of preload and possible damage enhancement. In conjunction with the above investigations, fatigue and tensile tests will be performed on damaged and undamaged specimens to establish the effect of impact on these properties.

Damage base data will be generated using nominal thickness fabricated specimens (the leading edge thickness will be identical to the corresponding blade type at the 50% span level). Half-thickness fabricated specimens will then be used in a scaling effects investigation. Preload investigations will be performed on the fabricated metal specimens to simulate the effects of centrifugal loading on local leading edge damage. The specimens will be preloaded at stresses typical of the impact locations (30 and 70% span levels).

6.2.3 Metal Specimen Tests

The impactors for the metal specimen tests include 1.5-pound birds, 1-inch diameter ice spheres, 1-inch diameter by 4-inch long ice cylinders, 0.062 and 0.125-inch diameter steel spheres and 1/4-inch diameter pebbles.

The impact velocities that will be used for the metal specimens correspond to those which would be typical of an impact at the 70% span and at the 30% span at full power settings of the engine during takeoff on each of the metal blade types (refer to Table 1). Impacts at 70% span are representative of the highest velocity impacts experienced by a blade. Impacts at 30% span are typical of those in the highest stress regions of the blade where it is most vulnerable to the effects of impact degradation.

The hard body impact tests on the nominal and half-scale thickness strainless steel fabricated specimens have been completed. The soft-body projectile impact testing using 3-ounce microballoon gelatin birds was initiated for the stainless steel specimens.

6.2.4 Composite Specimen Tests

6.2.4.1 Laboratory Size Composite Specimen Tests

Fabricated B/Al composite specimens that simulate the leading edge of the APSI blade at 50% span will be tested. One impact velocity that corresponds to that typical of an impact at the 70% span location of the APSI B/Al blade at the takeoff power setting will be used (refer to Table 1). In the damage data base study, data will be obtained for two sizes (0.062 and 0.125-inch diameter) of steel sphere impactors. In the scale effects investigation, data will be obtained only with the 0.062-inch steel sphere impactor. No testing is planned in regard to preload effects, since insignificant effect of preload was experienced for center panel impacts onto composite specimens in a previous investigation. Seven undamaged specimen tests will be used to provide a data base for the residual property measurements. A total of 22 fabricated B/Al composite specimens will be used.

6.2.4.2 Full-Scale Composite Blade Tests

In addition to testing laboratory size specimens, full-scale composite blades will also be impact tested. The local leading edge damage problem will be investigated by conducting hard impactor impacts on the leading edge of three B/Al APSI blades. The hard impactors utilized in the testing will be 0.25-inch diameter pebbles, 0.062-inch diameter steel spheres, and 0.125-inch steel spheres. Multiple impacts along the leading edge of the real blades will allow determination of the ballistic limit and provide qualitative damage data for the three sizes of hard impactors.

Full-scale composite blade testing will also be conducted to investigate structural damage resulting from soft body projectile impacts. Four B/Al APSI blades will be impacted using either 3-ounce microballoon gelatin birds or 1-inch diameter ice spheres. The blades will be impacted at the 30 and 70% span locations at velocities and impact angles corresponding to the span location.

6.3 SUBTASK C - MATERIAL SCREENING TESTS

6.3.1 Introduction

This subtask addresses the development of material screening tests necessary to evaluate and effectively rank candidate materials for fan and compressor blades that possess superior FOD resistance. The material parameters that will be investigated in this study include: (1) the perforation resistance of the material; (2) the extent the material may plastically deform; (3) the extent to which the material is vulnerable to catastrophic structural failure; and (4) the extent to which the material is vulnerable to degradation of fatigue properties.

In this investigation, it is planned to define these material parameters in terms of response to impact in small-scale tests. The perforation resistance material parameter will be quantified as a ballistic limit velocity, V_L , for a given impact configuration. The quantity V_L is a direct measure of the amount of impact energy which the material can absorb without catastrophic local damage. The plastic deformation parameter will be quantified by conducting impact tests which maximize the likelihood of plastic deformation. The catastrophic structural failure material parameter will be quantified in a Charpy impact test designed to produce gross structural failure. The fatigue properties parameter will be quantified in terms of reduction of ultimate fatigue strength. The parameters defined by these tests may be considered individually or combined with suitable weighting functions to compute an overall figure of merit for a particular material.

6.3.2 Materials to be Investigated

The usefulness of material ranking by the screening tests will be evaluated by applying the tests to six materials. Three of the materials will be studied extensively in the overall program. These include 403 stainless steel used in J79 Stage 1 compressor blades, 8-1-1 titanium used in F101 Stage 1 fan blades, and boron/aluminum used in APSI Stage 1 fan blade. Additional materials to be tested include a heat treated 403 stainless steel, 6Al-4V titanium, and a graphite epoxy composite. All of the specimens (metal and composite) have been fabricated.

6.3.3 Screening Tests

6.3.3.1 Ballistic Limit Testing

This test will evaluate the ballistic limit velocity (V_L) for normal impacts of various typical FOD projectiles. Three impactors will be used in the testing. A 1/2-inch diameter microballoon gelatin sphere with 10 to 15% porosity will be utilized on all six materials for bird simulation. The remaining two impactors are 1/2-inch ice balls and 1/4-inch diameter stones or "standard" pebble. Both ice and stone impacts will be used on two of the metals which will be studied extensively in the overall program. These will be the 403 stainless steel and the 8-1-1 titanium. Pebble impacts will also be conducted on the boron/aluminum composite specimens; however, ice impacts will not be conducted since ice is believed to behave similar to the substitute bird material (microballoon gelatin). A total of 25 composite specimens will be used for ballistic limit testing. The launch velocity of the impactors will be varied until the ballistic limit (V_L) is determined within about 5%.

A number of ballistic limit tests (using the granite pebble) has been conducted on the metal and composite specimens. The ballistic limit of the 403 stainless steel was determined to be about 3375 feet per second for the 1/4-inch diameter granite pebbles. The ballistic limit for pebble impacts on

the boron/aluminum specimens was determined to be about 620 feet per second. Thus, the ballistic limit of stainless steel is five times greater than for boron/aluminum for pebble impacts.

6.3.3.2 Maximum Deformation Testing

Specimens that are identical to those used in the ballistic limit test will be utilized in the maximum deformation testing. The specimens will be impacted by 1/2-inch diameter microballoon gelatin birds (substitute bird material) to maximize plastic deformation of the target. Again, normal impacts in the specimen center will be utilized. The velocities will also be varied to collect data such that a plot of the deformation damage versus velocity can be made. It is believed that the maximum deformation damage will occur at a velocity just below the ballistic limit velocity (V_L), probably $0.9 V_L$.

The results of the local leading edge damage effort should provide a basis for selecting the most diagnostic damage parameter to use in measuring the damage. Two likely candidates are the plastically deformed area and maximum deflection. A total of 10 composite specimens will be used for maximum deformation testing.

6.3.3.3 Gross Structural Damage Testing

This test is designed to assess vulnerability to catastrophic structural damage of blades by using test specimens from the six candidate materials. Such damage is probably due to bending stresses at the root or some other mode on an impacted blade. The results of failure mode tests from previous tasks of the overall program will clarify this point. It is anticipated that an instrumented Charpy impact test will be sufficient to characterize material response to this type of loading. A total of eight composite specimens will be used.

6.3.3.4 Fatigue Testing

The fatigue strength test is an attempt to classify damage to specimens in terms of an equivalent stress concentration factor. Holes and cracks will be machined in specimens using the electrical discharge machining technique (EDM). The holes (0.177-in. diameter) and cracks (0.177-in. long) will be machined in the center of the specimen at its midspan. The damaged specimens will then be tested in a tensile fatigue machine. Each group of specimens with identical damage will be tested in the fatigue machine at load levels to obtain failure in the range from 10^4 to 10^5 cycles. The number of cycles to failure (complete separation) will be recorded for each specimen. The data will be plotted in the form of net section average stress against number of cycles to failure for each group of specimens. One or two specimens of each group will be used to obtain the residual tensile strength for baseline purposes. A total of 24 composite specimens will be used.

7.0 TASK V - PARAMETRIC ANALYSIS

7.1 INTRODUCTION

Parametric relationships describing the changes in dynamic structural response of impacted simple plate elements with the progressive introduction of blade airfoil geometric features will be derived in this task. Additionally, the adequacy of the structural response models formulated in Tasks II, III, and IV will be investigated and modifications made as necessary.

This task is broadly divided into three phases. The first phase is analysis and correlation of Task VI tests conducted with simple cantilevered flat plates with different aspect ratios and thicknesses. The second phase is the analysis and correlation of Task VI tests with geometry and impact conditions which are more representative of actual airfoil FOD dynamics but which are still simple enough that the sources of observed effects can be isolated. The third and final phase of this task is the analysis and correlation of Task VI and Task IX tests of the three selected first-stage airfoils in stationary and rotating environments.

7.2 BLADES SELECTED FOR ANALYSIS

The three first-stage blades selected are representative of first-stage airfoils from Air Force inventory, production development, and advanced development engines. These blades include subsonic, transonic, and supersonic airfoil shapes and stainless steel, titanium, and an advanced composite material. The blades selected are listed below:

<u>Blade</u>	<u>Representing</u>	<u>Airfoil</u>	<u>Material</u>	<u>Shrouded</u>
J79	Air Force Inventory	Subsonic	Stainless Steel	No
F101	Production Development	Transonic	Titanium	Yes
APSI	Advanced Development Supersonic Engines	Supersonic	B/Al Composite	No

7.3 PARAMETRIC MATRIX

A parametric matrix has been formulated to define the impact conditions and response model geometries that will be analyzed in Tasks V and X and provide guidance in the selection of the structural element and full-scale blade tests that will be conducted in Tasks VI, IX and XI. This matrix is shown in Table 5.

Table 5 describes the structural elements, element fixity and material, the analysis level, the loading and impactor, and the impact location and incidence. The analysis level in Table 5 refers to the transient structural

Table 5. Parametric Matrix Defining Structural Elements and Impact Conditions to be Analyzed.

- For each structural element/speed condition, initial analyses performed will be to determine first three natural frequencies and mode shapes.
- Structural elements are cantilevered except where additional fixity provided by shroud restraint is indicated.
- Structural elements have zero rotational velocity unless otherwise indicated.
- Structural element shape, size, and configuration details defined in Table II.
- Analyses correspond to room temperature, except as indicated by *, where a temperature of 300°F will be used.
- Analysis level 1 = NONIAP code, analysis level 2 = COMET code.
- Impact velocities of projectiles will be varied to obtain no damage to severe damage.
- Loading/impactors - unit impulse
 - M_{b1} 3-ounce bird
 - M_{b2} 1½-pound bird
 - M_{b3} 2-inch ice ball
 - M_{b4} slab ice

Group	Structural Element and Comments	Analysis Level	Loading/Impactor	Impactor Location	Impact Incidence	Shroud Restraint	Specimen Material	Task
1	Plate with blade-type aspect ratio. Natural freq.-mode shapes	1 & 2	NA	NA	NA	NA	Ti 6-1-1	V
2	Same as group 1, except impact analysis	"	Unit impulse	Center impact @ 70% span	Normal	"	"	"
3	"	"	M_{b1}	"	"	"	"	"
4	"	"	M_{b3}	Center impact @ 10% span	"	"	"	"
5	"	"	M_{b1}	Edge impact @ 70% span	Oblique	"	"	"
6	Plate with ½ blade type aspect ratio. Natural freq.-mode shapes	2	NA	NA	NA	"	"	"
7	Same as group 6, except impact analysis	"	M_{b1}	Center impact @ 70% span	Normal	"	"	"
8	"	"	M_{b2}	Edge impact @ 30% span	Oblique	"	"	"
9	Plate with blade type aspect ratio and ½ blade type thickness/chord ratio. Natural freq.-mode shapes	1 & 2	NA	NA	NA	"	"	"
10	Same as group 9, except impact analysis	"	M_{b1}	Center impact @ 70% span	Normal	"	"	"
11	Plate with blade type aspect ratio and tapered cross section. Nat. freq.-mode shapes	2	NA	NA	NA	"	"	"
12	Same as group 11, except impact analysis	"	M_{b1}	Edge impact @ 70% span	Oblique	"	"	"
13	"	"	M_{b2}	"	"	"	"	"
14	Plate with blade-type aspect ratio and airfoil like cross section. Nat. freq.-mode shapes	"	NA	NA	NA	"	"	"
15	Same as group 14, except impact analysis	"	M_{b2}	Edge impact @ 70% span	Oblique	"	"	"
16	Same as group 14, except with tip clamped	"	NA	NA	NA	Yes	"	"
17	Same as group 16, except impact analysis	"	M_{b1}	Center impact @ 70% span	Normal	"	"	"
18	F101 blade with clamped shrouds. Nat. freq.-mode shapes	1 & 2	NA	NA	NA	"	"	"
19	Same as group 18, except impact analysis	"	M_{b1}	Edge impact @ 70% span	Oblique	"	"	"
20	"	2	M_{b2}	Edge impact @ 10% span	"	"	"	"
21	F101 blade at 7550 rpm with clamped shrouds. Nat. freq.-mode shapes	1 & 2	NA	NA	NA	"	Ti 6-1-1	"
22	Same as group 21, except impact analysis	"	M_{b2}	Edge impact @ 70% span	Oblique	"	"	"

Table 5. Parametric Matrix Defining Structural Elements and Impact Conditions to be Analyzed (Continued).

Group	Structural Element and Comments	Analysis Level	Loading/Impactor	Impactor Location	Impact Incidence	Shroud Restraint	Specimen Material	Task
23	Same as group 21, except impact analysis	2	M _{b4}	Edge impact @ 70% span	Oblique	Yes	Ti 8-1-1*	V
24	F101 blade at 7550 rpm with shroud springs. Nat. freq.-mode shapes	1 & 2	NA	NA	NA	"	"	X
25	Same as group 24, except impact analysis	"	M _{b2}	Edge impact @ 70% span	Oblique	"	"	"
26	F101 blade sector at 7550 rpm. Nat. freq.-mode shapes	2	NA	NA	NA	"	"	"
27	Same as group 26, except impact analysis	"	M _{b2}	Edge impact @ 70% span	Oblique	"	"	"
28	"	"	M _{b4}	"	"	"	"	"
29	Same as group 24, but with modified blade geometry. Nat. freq.-mode shapes	"	NA	NA	NA	"	"	"
30	Same as group 29, except impact analysis	"	M _{b2}	Edge impact @ 70% span	Oblique	"	"	"
31	Plate with blade type aspect ratio. Nat. freq.-mode shapes	"	NA	NA	NA	No	403 stainless steel	V
32	Same as group 31, except impact analysis	"	M _{b2}	Edge impact @ 70% span	Oblique	"	"	"
33	Cambered plate with blade type aspect ratio. Nat. freq.-mode shapes	"	NA	NA	NA	"	"	"
34	Same as group 33, except impact analysis	"	M _{b2}	Edge impact @ 70% span	Oblique	"	"	"
35	Cambered twisted plate with blade type aspect ratio. Nat. freq.-mode shapes	1 & 2	NA	NA	NA	"	"	"
36	Same as group 35, except impact analysis	"	M _{b2}	Edge impact @ 70% span	Oblique	"	"	"
37	J79 blade. Nat. freq.-mode shapes	"	NA	NA	NA	"	"	"
38	Same as group 37, except impact analysis	"	M _{b2}	Edge impact @ 70% span	Oblique	"	"	"
39	"	2	M _{b3}	Edge impact @ 30% span	"	"	"	"
40	J79 blade at 7460 rpm. Nat. freq.-mode shapes	1 & 2	NA	NA	NA	"	403 stainless steel*	"
41	Same as group 40, except impact analysis	"	M _{b2}	Edge impact @ 70% span	Oblique	"	"	"
42	"	2	M _{b4}	Edge impact @ 30% span	"	"	"	"
43	Same as group 40, but with modified blade geometry. Nat. freq.-mode shapes	"	NA	NA	NA	"	"	"
44	Same as group 43, except impact analysis	"	M _{b2}	Edge impact @ 70% span	Oblique	"	"	"
45	Cross ply panel with blade type aspect ratio. Nat. freq.-mode shapes	1 & 2	NA	NA	NA	"	B/AL	"
46	Same as group 45, except impact analysis	"	Unit impulse	Center impact @ 70% span	Normal	"	"	"
47	"	"	M _{b1}	Edge impact @ 70% span	Oblique	"	"	"
48	Cross ply panel with 1/4 blade type aspect ratio. Nat. freq.-mode shapes	2	NA	NA	NA	"	"	"
49	Same as group 48, except impact analysis	"	M _{b1}	Edge impact @ 70% span	Oblique	"	"	"
50	Cross ply panel with blade type aspect ratio and 1/4 blade type thickness to chord ratio. Nat. freq.-mode shapes	"	NA	NA	NA	"	"	"
51	Same as group 50, except impact analysis	"	M _{b1}	Edge impact @ 70% span	Oblique	"	"	"
52	Cross ply panel with blade type aspect ratio and tapered cross section. Nat. freq.-mode shapes	"	NA	NA	NA	"	"	"
53	Same as group 52, except impact analysis	"	M _{b1}	Edge impact @ 70% span	Oblique	"	"	"
54	Cross ply panel with blade type aspect ratio & airfoil like cross section. Nat. freq.-mode shapes	1 & 2	NA	NA	NA	"	"	"
55	Same as group 54, except impact analysis	"	M _{b1}	Edge impact @ 70% span	Oblique	"	"	"

Table 5. Parametric Matrix Defining Structural Elements and Impact Conditions to be Analyzed (Concluded).

Group	Structural Element and Comments	Analysis Level	Loading/ Impactor	Impactor Location	Impact Incidence	Shroud Restraint	Specimen Material	Task
56	Cross ply panel with blade type aspect ratio and camber Nat. freq.-mode shapes	2	NA	NA	NA	No	B/AL	V
57	Same as group 56, except impact analysis	"	M _{b1}	Edge impact @ 70% span	Oblique	"	"	"
58	Cross ply panel with blade type aspect ratio & camber & twist. Nat. freq.-mode shapes	1 & 2	NA	NA	NA	"	"	"
59	Same as group 58, except impact analysis	"	M _{b1}	Edge impact @ 70% span	Oblique	"	"	"
60	APSI blade. Nat. freq.-mode shapes	"	NA	NA	NA	"	"	"
61	Same as group 60, except impact analysis	"	M _{b1}	Edge impact @ 70% span	Oblique	"	"	"
62	"	2	M _{b3}	Edge impact @ 30% span	"	"	"	"
63	APSI blade at 17500 rpm. Nat. freq.-mode shapes	1 & 2	NA	NA	NA	"	B/AL*	"
64	Same as group 63, except impact analysis	"	M _{b1}	Edge impact @ 70% span	Oblique	"	"	"
65	"	2	M _{b4}	Edge impact @ 30% span	"	"	"	"
66	Same as group 63, but with modified blade geometry. Nat. freq.-mode shapes	"	NA	NA	NA	"	"	"
67	Same as group 66, except impact analysis	"	M _{b1}	Edge impact @ 70% span	Oblique	"	"	"

response computer code; Level 1 is the finite element model based on the NOSAPM program, and Level 2 is the component element model based on the COMET program. Analyses of the same structural model with the Level 1 and Level 2 analyses are indicated in Table 5 for a number of cases. If the agreement between the Level 1 and Level 2 analyses proves to be exceptionally good, then the number of Level 1 analyses may be reduced.

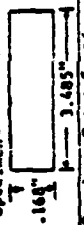


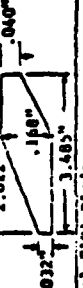
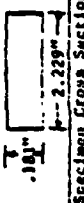


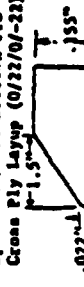
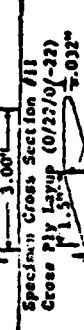
Table 5 includes a description of the structural models and impact conditions that will be used in Task X. In Task X, Full Stage Response Predictions, the response of a full stage of blades will be predicted. In this case, it is assumed that the only mechanical coupling is through shroud-to-shroud interaction and the models will include a single blade with the shrouds represented by springs and a sector of shrouded blades. The blades used in these models will be the F101 tip shrouded titanium first stage fan blades rotating at the take off angular velocity of 7550 rpm.

Details of the shape, size and configuration of the structural elements are provided in Table 6.

7.4 MODELING OF THE STRUCTURAL SPECIMENS

A study has been initiated to consider several of the options open to the user of the first level response analysis code (NOSAPM) which have a bearing on the accuracy of the program's results. One of the options available to the user is the number of nodes he chooses to describe the geometry and the displacement field of the three dimensional finite elements. A maximum of 21 nodes per element are available. Professor Bathe, the author of ADINA and consultant on this program, has suggested that 16 nodes be used, eliminating the mid-side nodes through the thickness. An initial comparison of these two element descriptions in the case of a static bending situation is made in Figures 19 and 20. The problem used for comparison is a cantilever plate loaded at its free end with a total force of 60 pounds distributed uniformly across its total width. The dimensions of the plate are 7 inches by 3 inches by 0.1875 inch, as shown in Figure 19. Four 20-noded elements were used in the finite element analysis of this problem, and the resulting bending stresses incurred at the top surface of the plate both along the centerline and at the $y = 1.5$ edge are plotted in Figure 19 as a function of z and compared with the beam analysis solution. The solutions are in good agreement except in the vicinity of the clamped end where the finite element analysis predicts an end effect. A second finite element analysis was then carried out using 16-noded instead of 20-noded elements, and the stress results of this analysis are compared against those obtained from the 20-noded element analysis in Figure 20. As can be seen from the figure, the agreement is quite close except in the vicinity of the clamped edge. Additional comparisons of these element descriptions will be subsequently carried out. Since elimination of four mid-side nodes through the thickness of each element will lead to substantial cost savings, the use of 16-noded elements should be closely considered.

Table 6. Shape, Size and Configuration Details of Structural Elements.

Groups	Specimen Span Length, in.	Specimen Cross Section	Specimen Material
1-5 6-8	12.250 6.125	Specimen Cross Section #1 	T1 B-1-1
9-10	12.250	Specimen Cross Section #2 	T1 B-1-1
11-13	12.250	Specimen Cross Section #3 	T1 B-1-1
14-17	12.250	Specimen Cross Section #4 	T1 B-1-1
18-20		Actual F101 Blade	T1 B-1-1
21-30		7101 Blade with Modified Geometry	T1 B-1-1
31-32	9.680	Specimen Cross Section #5 	403 Stain- less Steel
33-34	9.680	Specimen Cross Section #6 Same as Specimen Cross Section #5, but with Camber	403 Stain- less Steel
35-36	9.680	Specimen Cross Section #7 Same as Specimen Cross Section #6, but with Twist	403 Stain- less Steel
37-42		Actual J79 Blade	403 Stain- less Steel
43-44		J79 Blade with Modified Geometry	403 Stain- less Steel
45-47	6.10	Specimen Cross Section #8 Gross Ply Layout (0/22/0/-22)	B/AL
48-49	3.05		B/AL
50-51	6.10	Specimen Cross Section #9 Gross Ply Layout (0/22/0/-22) 	B/AL
52-53	6.10	Specimen Cross Section #10 Gross Ply Layout (0/22/0/-22) 	B/AL
54-55	6.10	Specimen Cross Section #11 Gross Ply Layout (0/22/0/-22) 	B/AL
56-57	6.10	Specimen Cross Section #12 Same as Specimen Cross Section #8, but with Camber	B/AL
58-59	6.10	Specimen Cross Section #13 Same as Specimen Cross Section #12, but with Twist	B/AL
60-65		Actual AP81 Blade	B/AL
66-67		AP81 Blade with Modified Geometry	B/AL

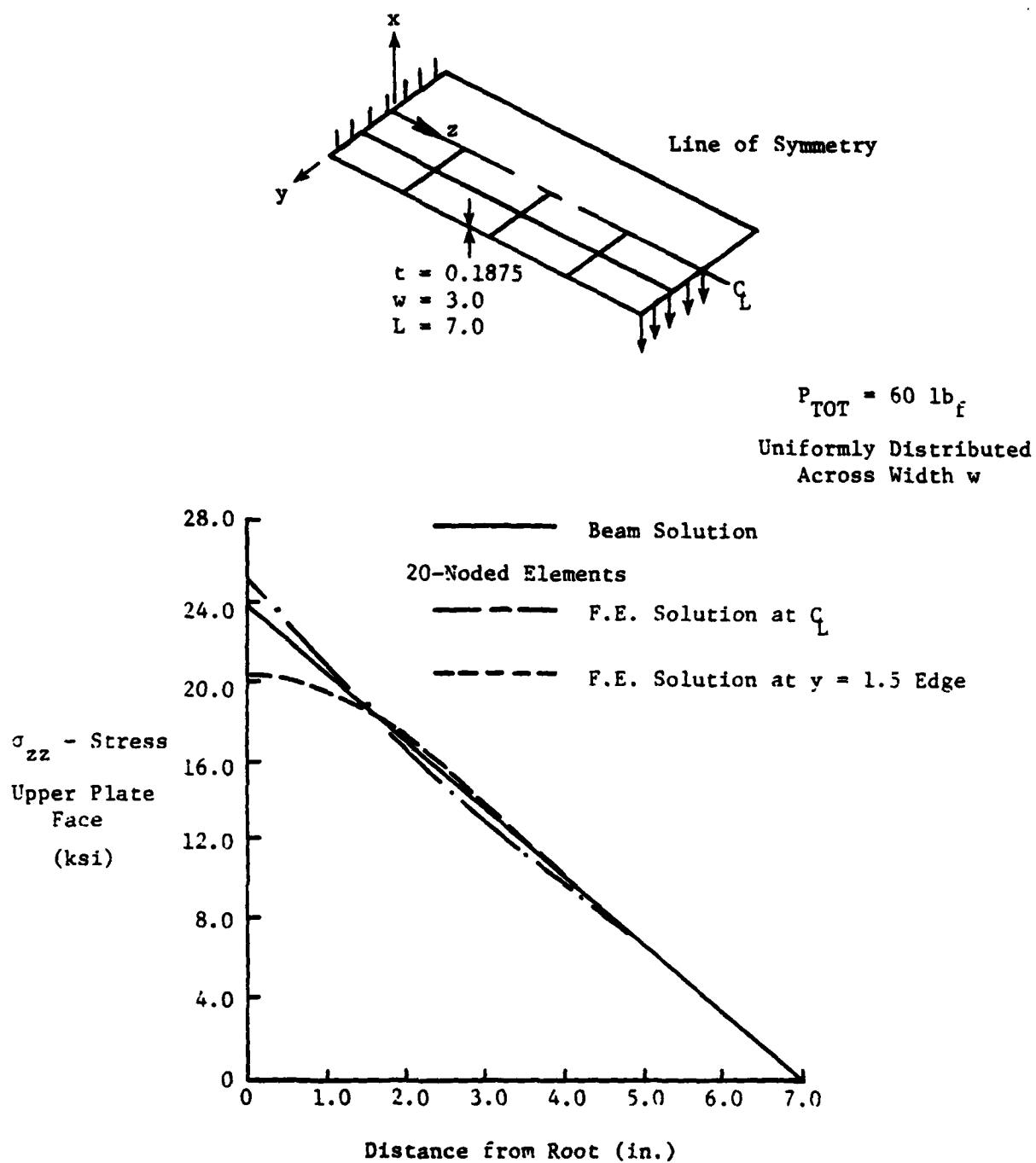


Figure 19. Comparison of 20-Noded Finite Element Solution with Beam Theory.

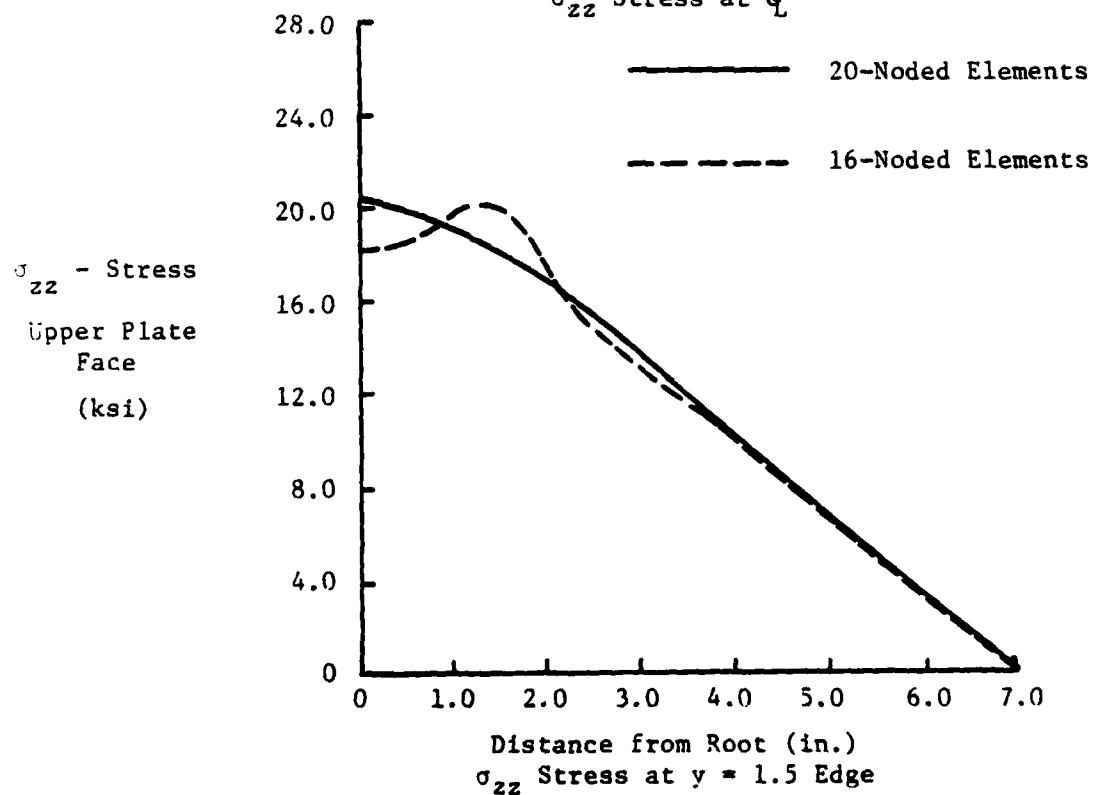
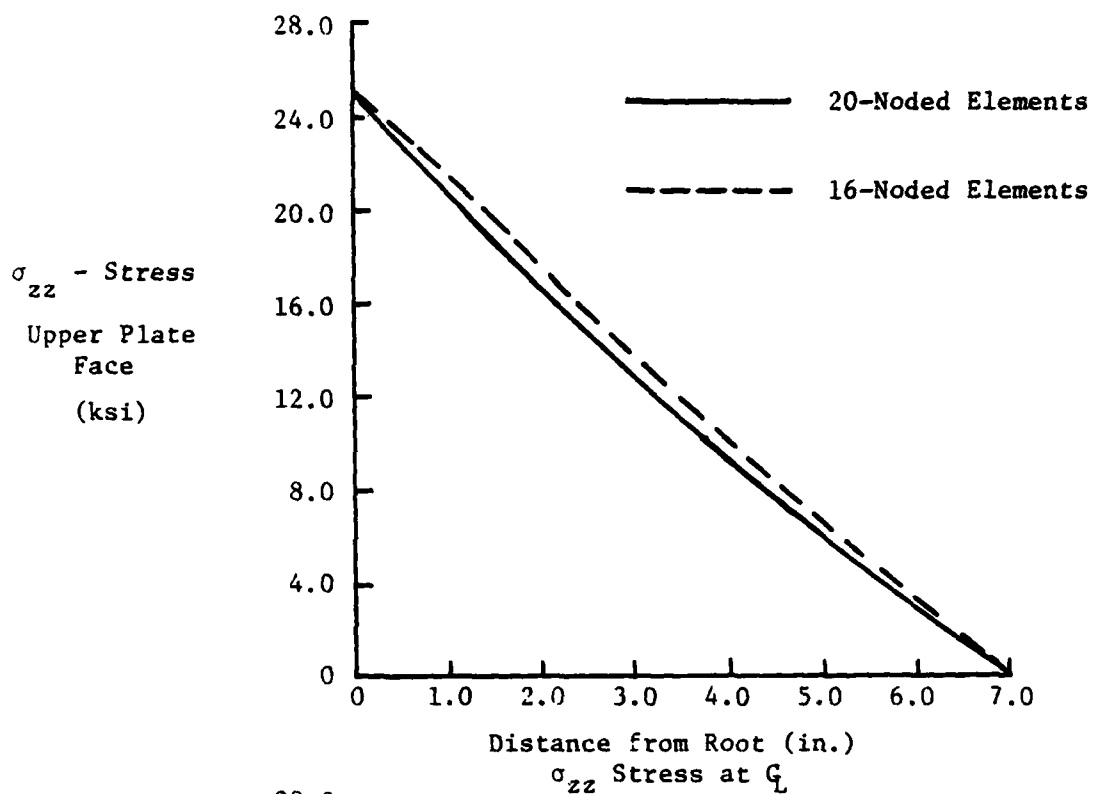


Figure 20. Comparison of 16-Noded Finite Element Solution with 20-Noded Element Solution.

In addition to this comparison, another study has been initiated to determine the number of elements that will be necessary to adequately model the plates and blades that will be tested in this program. The normal impact of a 0.0984-inch thick titanium plate (half the thickness representative of the F101 blade) is being considered. Various impact velocities of a 1-1/2-inch diameter, 3-ounce bird are being considered and subsequent blade responses studied.

8.0 TASK VI - STRUCTURAL ELEMENT TESTS

8.1 INTRODUCTION

The work of Task VI, "Structural Element Tests", is concerned with performing nonrotating bench impact tests on test specimens ranging from simple elements to real blades. The simple elements, such as beams and plates, will be tested with progressive introduction of airfoil geometric parameters to validate experimentally the analytical predictions of Task V and VIII. The purpose of Task V is to derive parametric relationships describing the changes in dynamic structural response as a function of material and geometric features. The purpose of Task VIII is to derive criteria for predicting blade foreign object impact damage tolerance. These criteria will be formulated to make full use of the transient dynamic analysis and experimental results obtained from other tasks of the program.

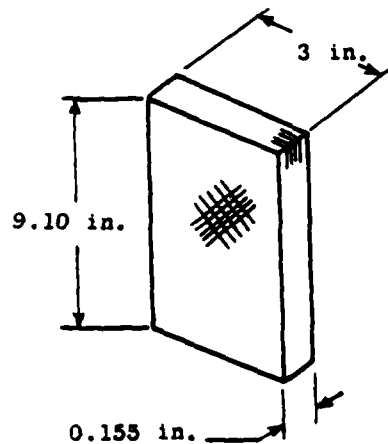
8.2 COMPOSITE SPECIMEN TESTS

8.2.1 Laboratory Size Composite Specimen Tests

The total number of fabricated B/Al specimens that will be tested is equal to 48. These specimens include flat panel, airfoil-like cross section, cambered, and cambered and twisted shapes. The test conditions are listed in Table 7 and the B/Al composite specimen configurations are shown in Figure 21.

Table 7. Task VI Fabricated Composite Specimen Test Conditions.

Velocities:	No Damage Threshold Damage Severe Damage	(3)
Impact Angle:	70% Span Location - Oblique 30% Span Location - Oblique	(2)
Impactor 2 to 3-Ounce Bird:	All Configurations Except Configuration 4	(6)
Test Conditions for 2 to 3-Ounce Bird Impacts - 36		
Impactor 2-Inch Ice Ball:	Configurations 6 and 7	(2)
Test Conditions for Ice Ball Impacts - 12		
Total Test Conditions - 48		



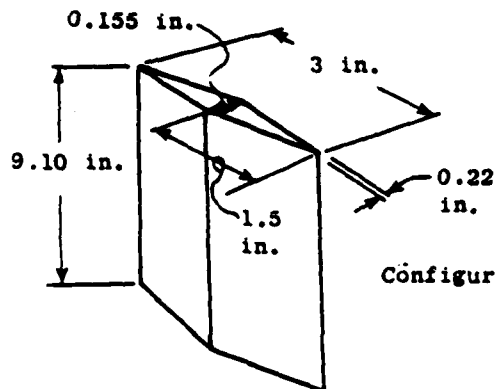
(a) Configurations 1, 2, and 3

Cross-Ply B/A1
(0/22/0/-22)

Configuration (1) - Blade Type Aspect Ratio Panel

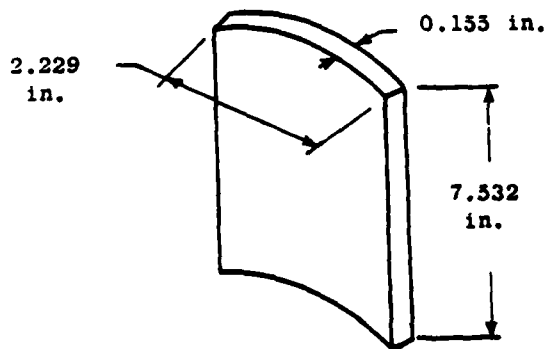
Configuration (2) - Same as (1), Except Length Reduced by 1/2

Configuration (3) - Same as (1), Except Thickness Reduced by 1/2



(b) Configuration 5

Configuration (5) - Airfoil-Like Cross Section Panel



(c) Configurations 6 and 7

J79 Specimen Die Used and Aspect Ratio Same as APSI

Configuration (6) - Cambered Panel

Configuration (7) - Same as (6). Except Twist Introduced After Forming

Figure 21. Task VI B/A1 Composite Test Specimen Configurations.

8.2.2 Full-Scale Composite Blade Tests

In addition to testing of laboratory size composite specimens, a number of tests will be conducted on the full scale B/Al APSI blades. The series of tests to be performed on real composite blades is outlined in Table 8.

Table 8. Task VI - Real Composite Blade Test Conditions.

Impact Parameters:	Mass - 2 to 3-Ounce Bird	(2)
	- 2-Inch Ice Ball	
	Velocity - No Damage	(3)
	- Threshold Damage	
	- Severe Damage	
	Location/Angle - 70% Span/Edge-Oblique	(2)
	- 30% Span/Edge-Oblique	
Test Conditions for Composite Blades		(12)

8.3 METAL SPECIMEN TESTS

Fabricated titanium 8Al-1Mo-1V and 410 stainless steel specimens and the corresponding blade types (F101 Stage 1 fan blade and J79 Stage 1 compressor blade) will be tested.

A baseline series of tests will be conducted on the titanium material and a supplementary series of tests will be conducted on the stainless steel. Titanium is chosen as the baseline material as it is the most common current blade material.

The baseline series of tests on the titanium material will consider all impact conditions and blade geometrical effects introduced progressively (not independently) except camber and twist. It has been established that camber and twist are not cold-formable on the titanium specimens and that these parameters could be incorporated only through hot forming or machining operations. Therefore, camber and twist will be investigated utilizing stainless steel specimens which will be cold formed.

Table 9 shows the test conditions for fabricated metal specimens and Table 10 shows the test conditions for the real metal blades.

During testing of the fabricated structural specimens, the different geometry effects (i.e., aspect ratio, thickness/chord ratio, etc.) will be introduced in a different sequence for the titanium and steel specimens so that any synergistic effects that might exist can be accurately assessed.

Table 9. Task VI - Fabricated Metal Specimen Test Conditions.

Baseline Test Conditions for Titanium

Impact Parameters:	Mass (All)	(3)
	Velocity (All)	(3)
	Location/Angle (All)	(2)
Blade Parameters:	All (Progressive) Except Camber and Twist. Also One Parameter at Elevated Temperature. Also Center and Edge Impact on Blade Type Aspect Ratio/Panels.	(8)
Test Conditions - 144		

Supplementary Series for Stainless Steel

Impact Parameters:	Mass - 1.5-Pound Bird	(2)
	- 2 to 3-Ounce Bird	
	Velocity - (All)	(3)
	Location/Angle - (All)	(2)
Blade Parameters:	Three Most Sensitive from Experiments on Titanium Plus Camber and Twist	(5)
Test Conditions - 60		

Table 10. Task VI - Real Metal Blade Test Conditions.

Impact Parameters:	Mass - 2 to 3-Ounce Bird	(3)
	- 1-1/2-Pound Bird	
	- 2-Inch Ice Ball	
	Velocity - All	(3)
	Location/Angle - All	(2)
Blades:	F101 (Shrouded)	(2)-Metal
	J79	Blades
Test Conditions for Metal Blades		(36)

9.0 TASK VII - ERROR BAND ANALYSIS

9.1 INTRODUCTION

The objective of this task is to analytically determine the uncertainties in strain history, deflection history, and damage-related parameters of FOD which are introduced by such factors as manufacturing tolerance, variability in material properties, and variability in impact conditions. This determination is important in Task VIII for quantifying variances for the damage model and in Tasks VI and IX for comparing computer output with test results.

The damage-related parameters will be among those used in Task VIII as the basis for the impact damage model, for example, maximum stress or maximum strain. These parameters will be obtained as output from the analysis models defined in Task II. It is expected that the second level response model will be adequate, but the detailed modeling required for studying the effects of local deviations in geometry within manufacturing tolerance might require the use of the first level analysis response model.

9.2 PROPERTIES REQUIRING AN ERROR BAND ESTIMATION

A list of properties relating to blade material, impactor characteristics, and aerogeometric factors for which the FOD design criteria developed in Task VIII will most need an error band estimation has been compiled. It is believed that variation of these properties within a reasonable range can cause a wide variation in damage resulting from foreign object impact. These error band properties and the associated damage modes are identified in the matrix shown on Table 11.

Table 11. Matrix of Error-Band Properties and Associated Damage Modes.

Damage Modes Error Band Properties	Metal Blades					Composite Blades					
	Stage to Stage In-terference	Mass Loss	Tear-ing	Large Plastic Deform.	Small Plastic Deform.	Stage to Stage In-terference	Mass Loss	Delami-nation	Fiber Failure	Cracking	Small Plastic Deformation
<u>Impact Para.</u>											
Weight		X	X	X	X		X				X
Location	X	X		X		X	X	X	X	X	
Duration	X			X		X			X	X	
<u>Aero/Geom-etric Para.</u>											
Tip Clear.	X					X					
Interstage and Stage to Stage Clear-ance	X					X					
Max. Thick.		X					X				
LE Thick.			X								
Thick. Dist-ribution		X		X			X				
<u>Material Parameters</u>											
Ductility	X	X	X	X		X	X				
Strain Rate		X	X	X			X		X	X	X
Yield Stress				X	X						
Surface Quality					X						X

10.0 TASK VIII - FOREIGN OBJECTIVE IMPACT DESIGN CRITERIA

10.1 INTRODUCTION

The purpose of this task is to derive the criteria for predicting blade foreign object impact damage tolerance. The criteria will be formulated to make full use of the transient dynamic analysis and experimental results obtained in the previous tasks and will be based on a combination of theory and regression analysis. Dimensional analysis and an examination of the physics of impact will determine which impact dynamics and airfoil response parameters will be used to formulate the damage model. Regression analysis will be used to determine the constants in the model by correlation with the experimental results. The experience gained at General Electric in the development of simplified criteria based on purely elastic analyses will provide an excellent basis for the complete elastic-plastic analysis of this program.

The damage models formulated will be correlated with the observed damage from Tasks VI and IX tests, and will each be sufficiently resolved to predict a threshold value beneath which the damage is not observed and above which the prescribed damage is evident. The level of damage for such definitions as local plastic deformation will be of relatively increasing severity from no damage to large plastic deformation so that multiple qualitative thresholds will be required. A more definitive damage criterion is to specify the size of the region of local plastic deformation relative to a normalizing dimension of the airfoil such as the chord. Damage definitions such as local fracture are qualitatively more precise measures so that a single threshold will be sufficient.

10.2 FOREIGN OBJECT IMPACT DESIGN CRITERIA GOALS

An initial list of foreign object impact design criteria goals has been compiled for consideration. For both metal and composite blades, these criteria include limits on overall blade displacement to avoid interference, limit on local plastic deformation to avoid stall/surge, and limits on the total distortion strain energy per unit volume to avoid mass loss. Additional criteria for composite blades include limits on the shear and through-the-thickness normal stresses to avoid delamination, and limits on the spanwise and chordwise normal stresses to avoid fiber failure.

Relative to metal blades, we are looking at an approach which appears very promising for predicting tearing that is based on the relative values of the maximum and minimum principal strains. This approach is based on a concept used in forming sheet metal where a forming limit diagram is used to determine whether a metal can be shaped without risk of failure or tearing.

11.0 REFERENCES

1. Storace, A.F., "Initial Research and Development Test Plan, Task I - Design System Structure," November 1977.
2. Description of the First and Second Level Analytical Models to be Used in FOD Studies, submitted to Air Force in a letter, A.L. Meyer to Lt. Paul Copp, AFAPL/TBP, December 5, 1977.
3. Levy, S. and Wilkinson, J., "The Component Element Method in Dynamics," McGraw-Hill, 1976.
4. Levy, S., "Pipe Whip Dynamics Including Pipe Yielding, Nonlinear Restraints and Variable Jet Force for 3D Systems," General Electric Corporate Research and Development Report No. 77CRD083, March 1977.
5. Wu, R., "Dynamic Analysis of Fuel Assemblies Including Fluid Effects," NEDM-21236, 76NED17, March 1976.
6. Barber, J.P., Wilbeck, J.S., and Taylor, H.R., "Bird Impact Forces and Pressures on Rigid and Compliant Targets," AFFDL-TR-60, November 1978.
7. 1977 Annual Book of ASTM Standards, Part 10 - Metal Physical, Mechanical, Corrosion Testing, pp. 154-173.
8. Structural Design Guide for Advanced Composite Applications, Volume I, Material Characterization - Test Methods, p. 7.3.5.
9. Chamis, C.C. and Sinclair, J.H., "Ten-Degree Off-Axis Test for Shear Properties in Fiber Composite," Experimental Mechanics, September 1977, pp. 39-346.
10. Krinke, D.C., Barber, J.P., and Nicholas, T., "The Charpy Impact Tests as a Method for Evaluating Impact Resistance of Composite Materials," UDRI-TR-77-54.